

# A CNN-based Prediction-Aware Quality Enhancement Framework for VVC

Fatemeh Nasiri, Wassim Hamidouche, Luce Morin, Nicolas Dholand, and Gildas Cocherel

**Abstract**—This paper presents a framework for Convolutional Neural Network (CNN)-based quality enhancement task, by taking advantage of coding information in the compressed video signal. The motivation is that normative decisions made by the encoder can significantly impact the type and strength of artifacts in the decoded images. In this paper, the main focus has been put on decisions defining the prediction signal in intra and inter frames. This information has been used in the training phase as well as input to help the process of learning artifacts that are specific to each coding type. Furthermore, to retain a low memory requirement for the proposed method, one model is used for all Quantization Parameters (QPs) with a QP-map, which is also shared between luma and chroma components. In addition to the Post Processing (PP) approach, the In-Loop Filtering (ILF) codec integration has also been considered, where the characteristics of the Group of Pictures (GoP) are taken into account to boost the performance. The proposed CNN-based Quality Enhancement (QE) framework has been implemented on top of the Versatile Video Coding (VVC) Test Model (VTM-10). Experiments show that the prediction-aware aspect of the proposed method improves the coding efficiency gain of the default CNN-based QE method by 1.52%, in terms of BD-BR, at the same network complexity compared to the default CNN-based QE filter.

**Keywords**—CNN, VVC, Quality Enhancement, In-Loop Filtering, Post-Processing

## I. INTRODUCTION

VIDEO codecs aim at reducing the bit-rate of compressed videos to decrease the traffic pressure on the transmission networks. As this process directly affects the perceived quality of received videos, the importance of retaining high quality displayed video becomes more evident. In particular, the emergence of new video formats, such as immersive 360°, 8K and Virtual Reality (VR), has pushed more pressure on further bandwidth saving in order to guarantee an acceptable quality. To address this problem, in recent years, besides the great improvements in the domain of transmission network technologies, the development of new video codecs and standards has been initiated. Notably, Versatile Video Coding (VVC) [1], AoM Video codecs (AV1 and AV2) [2] and Essential Video Coding (EVC) [3] are expected to bring a significant improvement in terms of bitrate saving over existing

video coding standards such as High Efficiency Video Coding (HEVC) [4].

Although the new video codecs benefit from more efficient algorithms and tools compared to the previous generation standards, reconstructed videos using these codecs still suffer from compression artifacts, especially at low and very low bitrates. The block-based aspect of the hybrid lossy video coding architecture, shared among all these codecs, is the main source of the blockiness artifact in reconstructed videos. To remove this type of artifact, a De-Blocking filter (DBF) has been used in most of existing codecs [1, 2, 4, 5]. DBF applies low pass filters in order to smooth out block borders and correct the discontinuous edges across them. Quantization of transform coefficients rather introduces other types of compression artifacts, such as blurriness and ringing. The larger the quantization step gets, the more visible the blurriness and the ringing become. The quantization step is controlled by Quantization Parameter (QP), which varies from 1 to 63 in VVC. In low bit-rate video coding, where higher QP values are used, the perceived quality is visibly degraded. Sample Adaptive Offset (SAO) and Adaptive Loop Filter (ALF) are additional filters that are mainly designed to overcome this problem. SAO categorizes reconstructed pixels into pre-trained classes and associates to them a set of optimized offsets to be transmitted for texture enhancement. ALF, that is applied after DBF and SAO in VVC, further improves reconstructed frames. In ALF, parameters of a set of low pass filters are optimized at the encoder side and transmitted to the decoder. The common aspect between all these methods is the hand-crafted nature of their algorithms. Although these methods significantly remove undesirable artifacts, the task of enhancing reconstructed videos still has room for further quality improvement.

The promising advances in the domain of machine learning have recently encouraged the broadcast industry to explore it in the video compression domain. Particularly, deep Convolutional Neural Networks (CNNs) have attracted more attention owing to their significant performance [6, 7]. Motivated by CNN-based approaches in other image processing tasks, such as Super Resolution (SR) and machine vision, several recent studies have been established in the domain of artifact removal from compressed videos. These approaches are categorized into two main groups: Post Processing (PP) and In-Loop Filtering (ILF). The Post Processing (PP) approach improves reconstructed videos after the decoding step and is considered flexible in terms of implementation, as it is not normatively involved in the encoding and decoding processes. In other words, such a PP algorithm serves as an optional step to be used based on the hardware capacity of decoder/receiver device. On the contrary, In-Loop Filtering (ILF) approach

F. Nasiri, W. Hamidouche and L. Morin are with University of Rennes 1, INSA Rennes, CNRS, IETR - UMR 6164, 35000 Rennes, France. (emails: {firstname.lastname}@insa-rennes.fr).

F. Nasiri, N. Dholand and G. Cocherel are with AVIWEST, Parc Edonia, Batiment X1, Rue de la Terre de Feu, 35760 Saint-Grégoire, France (emails: {ndholand, gcocherel}@aviwest.com).

F. Nasiri, W. Hamidouche and L. Morin are also with IRT b<>com, 35510 Cesson-Sévigné, France.

involves the normative aspect of encoding and decoding, by generating high quality reconstructed frames to be served as a reference to other frames in the prediction process.

In order to reduce artifacts and distortions in reconstructed videos, it is essential to take into account the source and the nature of the artifacts. Most studies have only used reconstructed video and corresponding original video as the ground truth for the training phase of their networks [8, 9]. Except for QP, which has a key influence on the distortion level, the use of other coding information is mostly overlooked in the existing studies. To further improve this aspect, in some more advanced works, coding information such as partitioning, prediction and residual information are also used [10–12]. However, these approaches are mainly applied to intra coded frames.

This paper presents a CNN-based framework for quality enhancement of compressed video. The key element of the proposed method is the use of prediction information in intra and inter coded frames. To this end, a prediction-aware Quality Enhancement (QE) method is proposed and used as the core module of two codecs integration approaches in VVC, corresponding to PP and ILF. In this method, separate models are trained for intra and inter coded frames to isolate the learning of their specific artifacts. The proposed framework emphasizes on the prediction type as critical coding information and offers frame-level as well as block-level granularity for enhancing the quality of reconstructed video pixels. The main contributions of this paper are summarized as follows:

- 1) Design and implementation of a complete framework for CNN-based quality enhancement based on frame-level and block-level prediction types in VTM-10.
- 2) Use of normative prediction decisions for training and testing of both intra and inter coding modes.
- 3) In inter frames, offering block-level granularity for distinguishing between enhancement task of intra blocks, inter blocks and skip blocks, using a block-type mask.
- 4) In-loop implementation of the proposed framework, using a normative frame-level signalling to deactivate CNN-based enhancement in case of quality degradation.
- 5) Finally, minimizing the memory requirement by sharing the QE models between all three colour components in all QP values.

The remaining of this article is organized as follows. Section II introduces the related works and categorizes them based on their contribution and relevance to this work. Section III presents details of the proposed prediction-aware QE method. This method is then used in Section IV as the core QE module in two codec integration approaches (PP and ILF). Experiment results are presented in Section V, and finally the paper is concluded in Section VI.

## II. RELATED WORK

In this section, some studies with significant contribution to the CNN-based video QE task are reviewed. As the proposed framework of this paper particularly focuses on the use of coding information, these studies are categorized and ordered to reflect how much they take into account the nature of compressed video signal and how their method exploits spatial

and temporal correlations for the QE task. Table I provides a list of the most relevant papers published in the past few years and summarizes their principle contributions, with a focus on the use of coding information.

### A. Single-Frame Quality Enhancement

Most CNN-based QE methods enhance the quality of video in a frame-by-frame manner, where each frame is enhanced independently. These methods exploit spatial information of texture pixels of individual frames in order to enhance their quality and remove their artifacts. One of the early works in this category, proposed in [13], uses a network with three convolutional layers to learn the residual information. This method is implemented as ILF and replaces SAO filter of HEVC. Another method called Deep CNN-based Auto Encoder (DCAD), deploys a relatively deeper network with ten layers to be used as a PP filter after decoding [15]. Inspired by the diversity of block sizes in HEVC, an ILF named Variable-filter-size Residue-learning CNN (VRCNN) proposes a network with different filter sizes to replace both SAO and DBF filters of HEVC intra coding [17]. The method presented in [30] enhances the performance of VRCNN by introducing more non-linearity to the VRCNN network. The added ReLU [62] and batch normalization [63] layers in this method improve its performance, compared to VRCNN.

In another work, presented in [19], two different networks are trained for intra and inter frames. The intra network is a sub-net of the inter network which helps the method to capture artifacts of intra coded blocks in P and B frames more efficiently. Furthermore, in [19], the complexity of the QE filter is controlled by comparison of a Mean Squared Error (MSE)-based distortion metric in the Coding Tree Unit (CTU) level at the encoder side. The Residual Highway CNN (RHCNN) network, presented in [23], is composed of several cascaded residual blocks, each of which having two convolutional layers, followed by a ReLU activation function. In RHCNN, inter and intra coded frames are also enhanced with dedicated networks. In [46], residual blocks in the network are enhanced by splitting the input frame and processing each part with a different CNN branches. The output of each branch is then concatenated and fed to the next block. As another contribution, a weighted normalization scheme is used instead of batch normalization which also improves the training process.

More recently, Multi-scale Mean value of CU-Progressive Rethinking Network (MM-CU-PRN) loop filter has been introduced [28] which uses progressive rethinking block and additional skip connections between blocks, helping the network to keep a longer memory during the training and be able to use low level features in deeper layers. MM-CU-PRN is placed between DBF and SAO filters and benefits from coding information by using multi-scale mean value of Coding Units (CUs). The network presented in [8], Multi-level Feature review Residual dense Network (MFRNet), deploys similar network architecture as in MM-CU-PRN. However, MFRNet utilizes multi-level residual learning while reviewing (reusing) high dimensional features in the input of each residual block which leads to a network with better performance compared to existing networks.

TABLE I: An overview of recently published CNN-based QE methods in the literature, with a summary of their contribution as well as the type of coding information they use (e.g. Transform Units Map (TUM) , Coding Units Map (CUM), Residual Map (ResM)), Prediction Map (PrM), Mean Map (MM), Intra Prediction Mode Map (IPMM) and Coding Type (CT). Moreover, the functionality (Func.) denotes whether a method is integrated in codec as ILF or PP.

Method	Published	Training dataset	Coding information	QE Func	Summary of contribution
IFCNN	IVMSP 16 [13]	CTC	QP	ILF	Applied after DB instead of SAO. 3 layers CNN with residual learning.
STRResNet	VCIP 17 [14]	AVS2	QP	ILF	After SAO, uses previous reconstructed block. 4 CNN layers with residual learning
DCAD	DCC 17 [15]	-	QP	PP	A 10 layers CNN network with residual learning.
DSCNN	ICME 17 [16]	BSDS500	QP	PP	Scalable network with separate branches for inter and intra frames
MMS-net	ICIP 17 [10]	Xiph.org	QP TUM	PP	Replaces all HEVC loop filters in intra coded frames. Scalable training.
VRCNN	MMM 17 [17]	-	QP	PP	Replaces HEVC in-loop filters in intra mode, variable CNN filter sizes.
MSDD	DCC 18 [18]	Youtube	QP	PP	Multi-frame input (next and previous frames) with multi-scale training
-	ICIP 18 [11]	-	QP PM MM	PP	Mean and partitioning mask with reconstructed frames are fed to a residual-based net.
QECNN	IEEE-TCSVT 18 [19]	BSDS500	QP	PP	Two networks with different filter sizes for inter and intra frames, time constrained QE
-	IEEE access 18 [20]	JCT-VC	QP	PP	Temporally adjacent similar patches are also fed to an inception-based net.
MFQE	CVPR 18 [21]	JCT-VC	QP	PP	Current and motion compensated frames of high quality adjacent frames are fed to net.
CNNF	ICIP 18 [22]	DIV2K	QP	ILF	QP and reconstructed frame are fed to network, replacing SAO and DBF.
RHCNN	IEEE-TIP 18 [23]	CTC	QP	ILF	QP-specific training of a network based on several residual highway units
FECNN	ICIP 18 [24]	BSDS500	QP	PP	A residual based network with two skip connections proposed for intra frames.
Residual-VRN	BigMM 18 [25]	MSCOCO	QP ResM PrM	PP	Prediction and quantized residual frame are fed to a residual based network as input.
MGANet	arXiv 18 [26]	Derf	QP TUM	PP	TUM is also fed to a multi-scale net. which exploits output of a temporal encoder.
ADCNN	IEEE access 19 [27]	DIV2K	QP TUM	ILF	Network composed of attentions blocks, using also QP and TU map.
MM-CU-PRN	ICIP 19 [28]	DIV2K	QP CUM	PP	Based on Progressive Rethinking Block which multi-scale CU maps are also used.
SDTS	ICIP 19 [29]	CTC	QP	PP	Multi frame QE scheme, using motion compensated frames and an improved network.
VRCNN-BN	IEEE access 19 [30]	-	QP	PP	Adds further non-linearity to VRCNN by adding batch normalization and Relu layers.
MIF	IEEE-TIP 19 [31]	HIF	QP CUM TUM	ILF	Selects high quality references to the current frame and exploits them in the QE.
-	APSIPA ASC 19 [12]	DIV2K	QP CUM TUM	PP	A network based on residual learning, exploiting TU and CU maps.
MRRN	IEEE SPL 19 [32]	BSDS500	QP	PP	Adopts a multi-reconstruction recurrent residual network for PP-QE task.
RRCNN	IEEE-TCSVT 19 [33]	-	QP	ILF	Intra , Recursive structure and Residual units with local skip connections
B-DRRN	PCS 19 [34]	-	QP CUM MM	PP	Network based on recursive residual learning, exploiting mean and boundary mask.
CPHER	ICIP 19 [35]	Vimeo	QP PrM	PP	Network based on residual blocks, exploiting unfiltered frame and prediction.
WARN	ICIP 19 [36]	DIV2K	QP	ILF	A wide activation residual network for ILF of AV1 codec.
ACRN	ICGIP 19 [37]	DIV2K	QP	ILF	Asymmetric residual network as ILF in AV1, with a more complex net. for higher QPs.
QG-ConvLSTM	ICME 19 [38]	-	QP	PP	Spatial features of distorted frame are combined with neighboring frames' features.
-	IEEE-TIP 19 [39]	Vimeo	QP	PP	Based on Kalman filters, using temporal information restored from previous frames.
SimNet	PCS 19 [40]	DIV2K	QP	PP	Depth of network is varied based on the distortion level.
LMVE	ICIP 19 [41]	-	QP	PP	Single and multi frame QE net. proposed, using FlowNet to generate high quality MC.
-	CVPR 19 [42]	DIV2K	QP	PP	Residual block based network which receives different scales of input frame.
SEFCNN	IEEE-TCSVT 19 [43]	DIV2K	QP CT	ILF	Optional ILF with adaptive net. selection for different CT and distortion levels.
DIANet	PCS 19 [44]	-	QP	ILF	Dense inception net. with different attention blocks, separating inter/intra frames.
-	IEEE-TIP 19 [45]	BSDS500	QP	ILF	Content-aware ILF with adaptive network selection depending on CTU content
MFRNet	arXiv 20 [8]	BVI-DVC	QP	ILF	An architecture based on multi-level dense residual blocks with feature review.
EDCNN	IEEE-TIP 20 [46]	CTC	QP	ILF	Network with enhanced residual blocks with weight normalization.
BSTN	MIPR 20 [47]	Derf SJTU	TUM MM	PP	MC frames along with distorted frame and additional coding information are fed to net.
FGTSN	DCC 20 [48]	-	QP	PP	Flow-guided multi-scale net. using motion field extracted from neighboring frames.
-	IEEE access 20 [49]	JCT-VC	QP	PP	Sparse coding based reconstruction frame fed to net. with MC and distorted frames.
-	ACM 20 [50]	CLIC	QP	PP	Fine-tuned QE network transmitting modified weights via bitstream.
FQE-CNN	IEEE-TCSVT 20 [51]	CLIC	QP IPMM	PP	Image size patches used for training, using intra modes map.
-	ICME 20 [52]	BVI	QP	PP	Post-processing for VVC encoded frames with network based on residual blocks.
RBQE	arXiv 20 [53]	RAISE	QP	PP	Blind QE with an easy-to-hard paradigm, based on dynamic neural net.
IFN/PQEN-ND	NC 20 [54]	SJTU	QP	ILF	Noise characteristic extracted from frames for enhancing intra and inter frames.
QEVN	ICCCS 20 [55]	CDVL,REDS	QP	ILF	Depending on motion, a selector network selects different networks for QE.
MSGDN	CVPRW 20 [56]	COCO2014	QP	PP	A multi-scale grouped dense network as a post-processing of VVC intra coding
PMVE	IEEE-TC 20 [57]	-	QP	PP	Frames are enhanced by contributing prediction info. from neighboring HQ frames.
MWGAN	arXiv 20 [58]	-	QP	PP	GAN multi-frame wavelet-based net., recovering high frequency sub-bands.
STFCNN	DCC 20 [59]	-	QP	PP	Multi-frame QE method with a dense residual block based pre-denoising stage
MPRNET	NC 20 [60]	BSD500	QP	PP	GAN multi-level progressive refinement, replacing the DBF and SAO in HEVC
RRDB	UCET 20 [61]	BSD500	QP	PP	A GAN-based network for QE of Intra coded frames of HEVC

Multi-Reconstruction Recurrent Residual Network (MRRN) is a method based on recursive learning and is implemented

as PP filter for decoded frames of HEVC [32]. In recursive learning, the same layers are repeatedly applied which reduces

the probability of over-fitting during the training. Likewise, in [33], another recursive residual network is proposed as ILF for intra coded frames. The proposed network in [33] is applied on reconstructed frames before the DBF and SAO filters. Block Information Constrained Deep Recursive Residual Network (BDRRN) is another method based on recursive residual learning in which a block-based mean-mask, as well as the boundary-mask, are used as input to network [34].

Furthermore, in some works, the focus is put on strategies for enhancing the quality of video frames. In [53], a blind quality enhancement approach is proposed where frames with different distortion levels are processed differently. An “easy-to-hard” QE strategy is used to determine which level of the CNN-based filtering shall be applied on a given frame. In the case that the quality is already satisfying based on a blind quality assessment metric, the QE process stops, otherwise, it continues. In Squeeze-and-Excitation Filtering CNN (SEFCNN) [43], an adaptive ILF is also proposed in which networks with various complexity levels are trained for different QPs.

### B. Multi-frame Quality Enhancement

Multiframe QE methods process a set of consecutive frames as input. The basic idea behind this category of methods is to remove the compression artifacts while considering the temporal correlation of video content. Moreover, the quality is propagated from frames encoded at high quality to adjacent frames encoded at lower quality.

One of the earliest implementations exploits temporal information simply by adding previously decoded frames to the input of the network, along with current frame [14]. In another method, Peak Quality Frames (PQFs) are detected with an SVM-based classifier [21]. Using a network named Motion Compensated (MC) sub-net, the MC frames of previous and next PQFs are generated. The three frames are then fed to another network, called QE sub-net, in order to enhance the quality of the current frame, while the selected PQFs are kept to be enhanced by another dedicated network. An improved version of this method has been introduced in [29, 64], where the high quality frame detection, as well as the QE network itself, are improved.

In multiframe QE methods, finding the best similar frames to the current frame for the task of motion compensation is important. In [31], similar reference frames with higher quality than the current frame are detected with a dedicated network. Then they are used to generate the MC frames with respect to the content of the current frame. This frame with computed motions is then used as input to the QE network along with the reconstructed frame. In another research, a flow-guided network is proposed, where the motion field is extracted from previous and next frames using FlowNet [48, 65]. Once the motion compensation is completed, a multi-scale network is applied to extract spatial and temporal features from the input. Following the same principle, motion compensated frames of adjacent frames are fed to network in [47]. A ConvLSTM-based network is then used to implicitly discover frame variations over time between the compensated adjacent

frames and the current frame. Moreover, in order to capture the texture distortion in compressed frames, the Transform Unit (TU) mean map is also fed to the network. In [49], in addition to the motion compensated frame, a sparse coding based reconstruction frame is also fed to the network as input. The purpose of using sparse coding prediction is to simplify the process of texture learning by the network. Similarly, in [20], most similar patches in previous and next frames are extracted and fed to a network with three branches of stacked convolutional layers. The branches are then concatenated to reconstruct the final patch.

Inspired by the multi-frame QE methods, a bi-prediction approach is proposed in [57]. In this work, instead of computing the motion field, a prediction of the current low quality frame is generated from neighbouring high quality frames. Then the predicted frame and reconstructed frame are fed to the QE network. In [58], a Generative Adversarial Network (GAN)-based multi-frame method is presented in which adjacent frames and current frame are fed to a GAN, which is itself composed of two parts: one for the motion compensation and the other for quality enhancement. Wavelet sub-bands of motion compensated frames and reconstructed frames are fed to the second part of the network as input. For evaluation of generated content, a wavelet-based discriminator that extracts features in the wavelet domain at several levels (*i.e.* sub-bands) is proposed.

In summary, multi-frame solutions adopt different motion compensation methods mostly based on block-matching or CNN-based approaches. However, they all overlook the fact that the actual motion modelling is performed based on a normative process which takes into account complex factors such as bitrate restriction or internal state of the encoder modules. In other words, one might consider the normative motion information available in the bitstream more useful than texture-based heuristic motion modelling. Furthermore, this signal is already available both at the encoder and decoder sides and can easily be used as side information for inference in the QE networks of PP and ILF methods.

### C. Methods based on coding information

In the literature, there are diverse levels of involving coding information in the CNN-training of the QE task. Here, we categorize these methods from the most basic coding information to the most advanced ones.

1) *Quantization Parameter (QP)*: A common basic coding information and one of the most useful ones is QP. Most of methods somehow involve the applied QP of the encoded signal in the training and the inference phases. There are mainly two approaches to use QP in CNN-based QE:

- QP-specific training: dedicating one model for each QP or a range of QPs [8, 66].
- QP-map training: providing QP as an input to the network [12, 27, 33, 50, 57].

Each approach has benefits and drawbacks. In the QP-specific training methods, the performance is usually higher as the artifacts of each QP have been particularly observed by their dedicated network during the training. However, they usually

require storing several trained models at the decoder-side which is not hardware-friendly. On contrary, QP-map methods are usually lighter to implement, especially when the QP value varies in finer granularity such as frame-level or block-level.

2) *Partitioning*: Another common coding information is block partitioning and boundary information. Depending on the flexibility of the codec under study (e.g. HEVC, AV1, VVC), this aspect is used differently in the literature. The simplest form of partitioning information is the boundary mask [11]. More sophisticated methods, especially HEVC-based ones, differentiate between Coding Units (CUs), Prediction Units (PUs) and Transform Units (TUs) boundaries [10–12, 27, 31, 34, 47].

3) *Prediction information*: Spatial and temporal prediction information has also been used for enhancement of coded videos. In [11], coding information such as the partitioning map as well as a mean-mask have been used as input to their proposed CNN-based QE network. The mean-mask is computed based on average reconstructed pixel values in each partition. In another work, presented in [35], a QE network is proposed in which the unfiltered frame and prediction frame are used along with the reconstructed frame as the input of the network. Finally, a three-level network composed of Inception and Residual Learning based Block (IResLB) units is proposed. The Inception and Residual Learning based Block (IResLB) units have three branches, each one having one to two convolutional layers. The intra mode map is then fed to the network to enhance the intra coded frames [51].

Regarding inter coding mode, an ILF with a selector network has been proposed in [55]. In this method, the selector network determines the motion complexity of a set of selected CUs and then decides whether to increase or decrease the QP value of CU and also which network (large or small scale network) to be used.

4) *Residual information*: Finally, the residual information has also been used as an additional input information for the task of encoded video enhancement. In [25], the coded residual information and prediction information are fed to a network to enhance intra coded frames in HEVC. The proposed network uses direct current (DC)-ReLU activation function in the first residual layer. The loss function in this work is a combination of Multi-Scale Structural SIMilarity (MS-SSIM), L1 and L2 functions. In another work, presented in [67], the QE task is modelled as a Kalman filtering procedure and enhance the quality through a deep Kalman network. To further improve the performance of the network, it uses prediction residuals as prior information.

To best of our knowledge, it is the first QE framework in which the spatial and temporal prediction information in frame and block levels are used for compressed video. In the following sections, the details of proposed framework are explained and integration in the VVC codec at both PP and ILF is presented.

### III. PROPOSED QUALITY ENHANCEMENT NEURAL NETWORKS

In this section, fundamental elements of the proposed prediction-aware QE method are described. A common net-

work architecture is adopted that takes into account prediction information associated with reconstructed image. This network is then trained separately for intra and inter images, and applied at the frame-level and block-level to both luma and chroma components, in order to enhance their content based on local coding types.

#### A. Network architecture

Recently there have been numerous studies on CNN-based architectures, improving their performance and complexity. In the literature, the residual blocks<sup>1</sup> have been widely used for super resolution and quality enhancement tasks which results in better enhancement and detail retrieval [68, 69]. Inspired by those works, the network architecture of this paper is based on residual blocks, combined with CNN layers, as shown in Fig 1. The first convolutional layer of the adopted network receives a single reconstructed signal as well as two associated coding information. In particular, a QP map and the prediction signal, both with the same size as the reconstructed signal, are concatenated with the reconstructed image as coding information. After one convolutional layer,  $N$  identical residual blocks, each composed of two convolutional layers and one ReLU activation layer in between, are used. The convolutional layers in the residual blocks have the same size as the feature maps and kernel size of the first convolutional layer. In order to normalize the feature maps, a convolutional layer with batch normalization is applied after the residual blocks. A skip connection between the input of the first and the last residual block is then used. Finally, three more convolutional layers after the residual blocks are used for reconstructing the enhanced reconstructed signal. Worthy of mention, the input size is arbitrary and not limited to one full frame. As will be explained later, depending on the granularity of the QE task, the inference might be applied in the frame-level or block-level.

Given  $\mathcal{I}$  as the concatenation of the input signals, the process of producing the enhanced reconstructed signal  $\hat{\mathcal{C}}$ , by the proposed CNN-based QE method is summarized as:

$$\hat{\mathcal{C}} = F_3^1(F_1^2(Bn^1(F_2^1(Res^N(F_1^1(\mathcal{I})))) + F_1^1(\mathcal{I})), \quad (1)$$

where  $F_1(\cdot)$  and  $F_2(\cdot)$  are  $3 \times 3 \times 256$  convolutional layers, with and without the ReLU activation layer, respectively. Moreover,  $F_3(\cdot)$  is a  $3 \times 3 \times 1$  convolutional layer with the ReLU activation layer. The superscript of each function indicates the number of times they are repeated sequentially in the network architecture. Finally,  $Res$  and  $Bn$  are the residual block and batch normalization layer, respectively.

Two different sets of inputs are used for the reference and the proposed methods. In the reference method, referred to as the prediction-unaware method in the rest of this paper, only the reconstructed  $\mathcal{C}$  and the QP map  $\mathcal{Q}$  are used, hence:

$$\mathcal{I}_{ref} = \mathcal{C} \oplus \mathcal{Q}, \quad (2)$$

<sup>1</sup>In the remaining of this paper, the term “residual” is occasionally used interchangeably in the context of video compression residual signal as well as neural network residual layer.

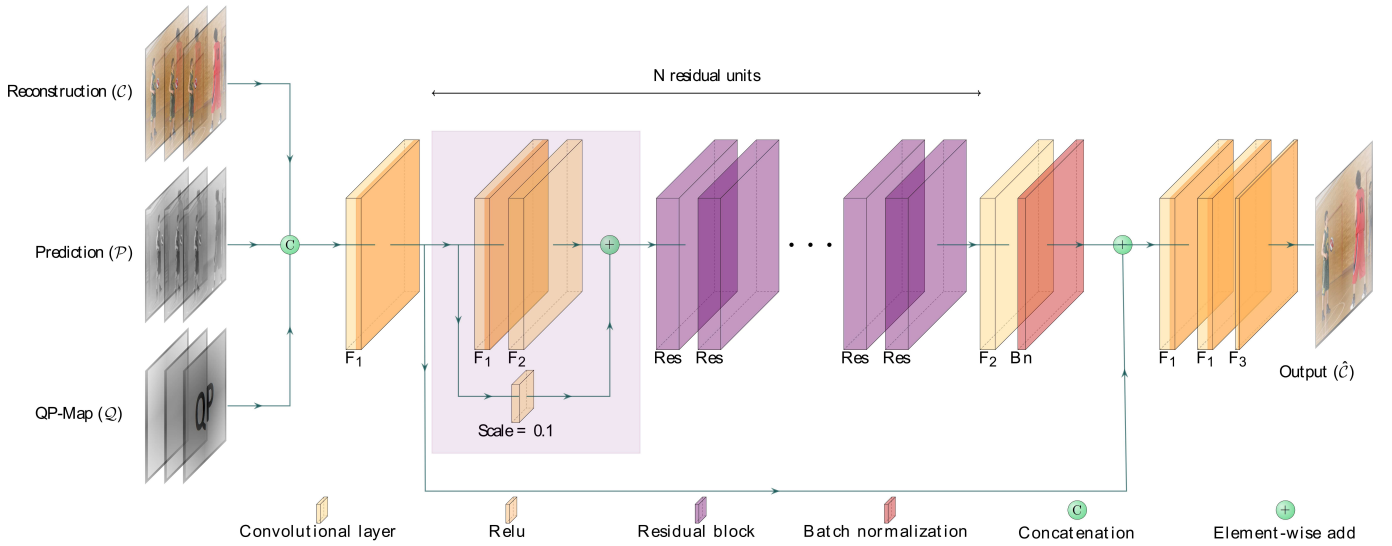


Fig. 1: Network architecture of the proposed method using the prediction, QP-map and reconstruction signal as the input.

where  $\oplus$  is the concatenation operator. Correspondingly, in the proposed method, referred to as the prediction-aware QE method, the prediction signal  $\mathcal{P}$  is also used:

$$\mathcal{I}_{pro} = \mathcal{P} \oplus \mathcal{C} \oplus \mathcal{Q}. \quad (3)$$

The normalized QP-map ( $\mathcal{Q}$ ) for a frame (or a block) with the width and height of  $W$  and  $H$ , respectively, is calculated as:

$$\mathcal{Q}_{i,j} = \frac{q_{i,j}}{q_{max}}, \quad (4)$$

where  $q_{i,j}$  is the QP value of the block that contains the pixel at coordinates  $(i, j)$ , with  $0 \leq i < W; 0 \leq j < H$ , and  $q_{max}$  is the maximum QP value (e.g. 63 in VVC).

Regardless of the QE method (*ref* or *pro*), the QE task can be summarized as:

$$\hat{\mathcal{C}} = f_{QE}(\mathcal{I}; \theta_{QE}), \quad (5)$$

where  $\theta_{QE}$  is the set of parameters in the network architecture of Eq. (1). This parameter set is optimized in the training phase, using the  $L_1$  norm as the loss function, computed with respect to the original signal  $\mathcal{O}$ :

$$L_1(\mathcal{O} - \hat{\mathcal{C}}) = |\mathcal{O} - \hat{\mathcal{C}}|. \quad (6)$$

### B. Prediction-aware QE

Even though the network architecture is common in the proposed method, signal  $\mathcal{P}$  is computed differently for intra and inter frames. Hence, different models are trained for each coding type in order to more efficiently learn their distortion patterns and based on their characteristics and functionality.

1) *Intra coded frames*: Intra coding is based on exploiting the spatial redundancies existing in frame textures. In VVC, a set of 67 Intra Prediction Modes (IPM), representing 65 angular IPMs, plus DC and planar modes are used for modelling texture of blocks. The selection of an IPM for a block is performed by optimizing the rate-distortion (R-D) cost, denoted as  $J_i$ :

$$J_i = D_i + \lambda R_i \quad i = 1, \dots, 67, \quad (7)$$

where  $D_i$  and  $R_i$  are the distortion and the rate of using the  $i^{th}$  mode, respectively. The Lagrangian multiplier  $\lambda$  is computed based on the QP which determines the relative importance of the rate and the distortion during the decision making process. In lower bitrates (higher QP values), the value of  $\lambda$  is higher, meaning that minimization of the rate is relatively more important than minimization of the distortion. Similarly, the opposite principle is applicable to higher bitrates (lower QP values).

The best IPM, minimizing the R-D cost of a block, is not necessarily the IPM that represents the block texture most accurately [66]. An example of such a situation is presented in Fig. 2. In this figure, a  $16 \times 16$  block,  $k$ , is selected and the prediction ( $\mathcal{P}_i^k$ ) and reconstruction ( $\mathcal{C}_i^k$ ) blocks corresponding to its two best IPMs in terms of R-D cost are shown. Precisely, these two best IPMs are angular modes 38 and 50. As can be seen, despite their similar R-D costs, these two IPMs result in very different reconstructed signals, with different types of compression loss patterns. On one hand, IPM 38 is able to model the block content more accurately (i.e. smaller distortion  $D_{38}$ ) at the cost of a higher IPM/residual signaling rate (i.e.  $R_{38}$ ). On the other hand, IPM 50 provides a less accurate texture modeling (i.e. high distortion  $D_{50}$ ) with a smaller IPM/residual signaling rate (i.e.  $R_{50}$ ). As a result, these two IPMs result in very different types of artifacts for a given block, as can be seen by comparing the corresponding reconstruction

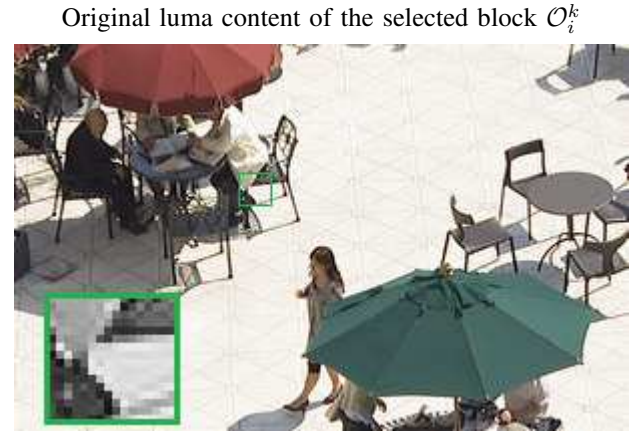
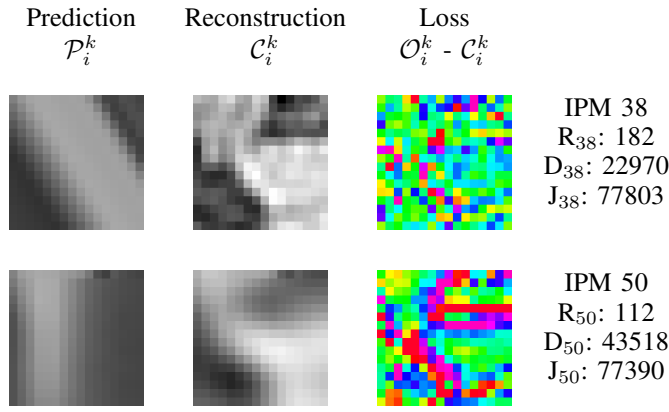


Fig. 2: An example of how two IPMs with similar R-D cost can result in different compression artifacts. The tested  $16 \times 16$  block,  $k$ , is coded with IPMs 38 and 50 in QP 40 with  $\lambda=301$ .

blocks (i.e.  $\mathcal{C}_{38}^k$  and  $\mathcal{C}_{50}^k$ ). This behavior is due to two different R-D trade-offs of the selected modes.

The above example proves that the task of QE for a block, frame or an entire sequence could be significantly impacted by different choices of coding modes (e.g. IPM) determined by the encoder. This assumption is the main motivation in our work to use the intra prediction information for the training of the quality enhancement networks.

The example in Fig. 2 proves that encoder decisions can have major impact on the QE task and its performance. Particularly, for intra blocks, we assume that the selected IPM for a block carries important information and shall be included in the training of the proposed CNN-based QE method [66]. Therefore, an intra prediction frame is constructed by concatenating the intra prediction signals in the block-level. This signal is then used as input to the network.

2) *Inter coded frames*: Inter coding is mainly based on taking advantage of temporal redundancy, existing in consecutive video frames. The prediction signal in the inter mode is a block, similar to the current one, selected from within the range of Motion Vectors (MVs) search, based on a distortion metric. In modern video codecs, we are allowed to search for such similar blocks in multiple reference frames. A motion compensated signal of a given frame, defined as a composition of the most similar blocks to the blocks of the current frame, is used as the prediction information signal in the proposed method. Fig. 3 visualizes how the prediction information signal is concatenated from reference frames. In this figure, current frame at time  $t$  uses four reference pictures, two from the past ( $t-1, t-2$ ) and two from the future ( $t+1, t+1$ ).

The temporal prediction signal usually provides additional texture information which is displaced with respect to the texture in the current frame. Hence, there is a potential benefit in using the additional texture information in the temporal prediction for CNN-based quality enhancement [70]. Moreover, in the hierarchical Group of Pictures (GoP) structure of the Random Access (RA) and Low Delay (LD) coding

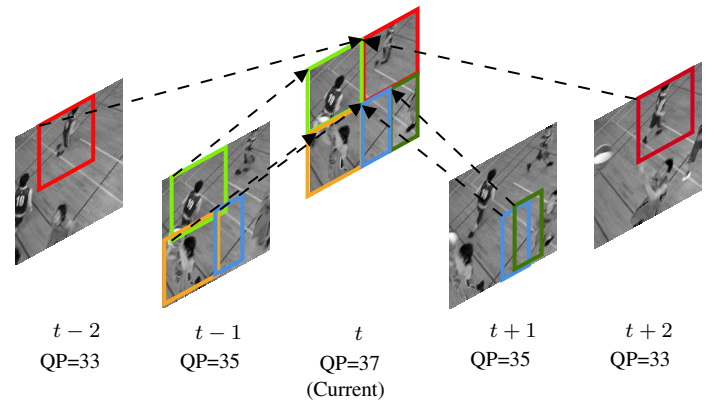


Fig. 3: An example of QP cascading in the hierarchical GoP structure, providing higher quality motion compensated blocks at frame  $t$  from past ( $t-1$  and  $t-2$ ) and future ( $t+1$  and  $t+2$ ) frames. Each block in frame  $t$  is predicted from at least one reference frame with lower QP (i.e. higher quality texture information).

configurations, these references are usually encoded using lower QP values than that of the current frame (Fig. 3). Therefore, for some local textures of the current frame, there could occasionally be a version of the texture in a higher quality due to the lower QP of its corresponding frame. The assumption of using the temporal prediction-aware QE method is that feeding the prediction information to the network makes it easier to model the heavily quantized residual signal and retrieve the missing parts in the current frame.

### C. Coding Type Granularity

1) *Frame-level*: In the two previous sections, we explained how the use of prediction information could improve the

performance of the QE task. The two trained networks for intra and inter are applied differently at the frame-level. In intra frames, since all blocks have the same coding mode and prediction type, the whole frame is enhanced using the intra trained network.

However, in inter frames, not all blocks have the same type of prediction. More precisely, three main prediction types can be found in blocks of an inter coded frame: inter, intra and skip. Fig. 4 shows an example of different block types within an inter coded frame. As a result, the prediction-aware quality enhancement of inter frames is performed in the block-level.

2) *Block-level*: The choice of the coding type of blocks in an inter coded frame depends on motion and texture characteristics. The regular inter mode, where the motion information along with residual signal is transmitted, is usually the more common type in inter coded frames. However, when the local content becomes too simple or too complex to compress, the skip mode and the intra mode might be used instead, respectively. More precisely, when a part of the video is static or has homogeneous linear motion, reference frames usually have very similar co-located blocks. In this case, skip mode is useful, where the motion is derived from neighbouring blocks and residual transmission is skipped. On contrary, due to fast motion or occlusion, sometimes no similar block can be found in reference frames. In this case, intra coding can offer a better prediction signal based on the spatial correlation of texture.

In the proposed QE scheme, blocks within inter coded frames are enhanced based on their coding type. To do so, a block-type mask is formed using the type information extracted from the bitstream. This mask is then used to determine the proper QE model for each block. Precisely, intra blocks and inter blocks are enhanced with intra-trained and inter-trained models, respectively. On contrary, skip blocks are enhanced using the prediction-unaware model, which is trained without any prediction information (See Eq. 2). When skip mode is signalled for a block, the content of prediction signal for that block is identical to the reconstructed block. As a result, the network which is trained with inter prediction signal and has learnt the motion in the video, is unsuitable for its enhancement. Our experiments showed that if identical prediction and reconstruction signals of skip blocks are fed to the proposed prediction-aware QE network, the performance will degrade, compared to the enhancement with the prediction-unaware method.

The implementation of the block-type mask can be performed at two levels: frame-level and block-level. In the frame-level application of the block-type mask, each inter frame is enhanced three times, using the trained networks for intra, inter and skip (prediction-unaware) coding types. Then, using the block-type mask of the frame, the three outputs are combined and one enhanced frame is produced. However, in the block-level application of the mask, the CNN-based QE is applied in the block-level, where each block is enhanced only once by using its appropriate model. Then all enhanced blocks are concatenated to form the final enhanced frame. Our experiments show that these two implementations have a negligible difference in terms of performance. Therefore, we chose to use the block-level approach, since it is significantly

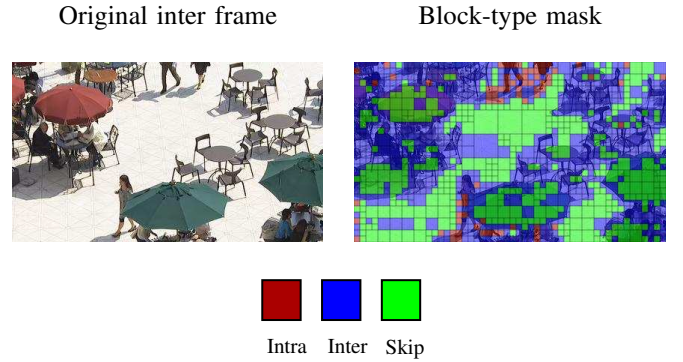


Fig. 4: Block type mask of an inter frame from the BQSquare sequence, with the three block types present.

less complex in terms of the number of operations than the frame-level implementation.

#### IV. CODEC INTEGRATION

The proposed QE method is integrated in the VVC codec with two different approaches: Post Processing (PP) and In-Loop Filtering (ILF). While their core QE modules share the same principles, described in the previous section, they possess unique characteristics and impose different challenges.

Fig. 5 shows where each codec integration method is placed and how it impacts the end-to-end system. In this figure, the green and blue modules represent the ILF and PP approaches, respectively, where only one of them can be activated in an end-to-end system. Also, removing both of them results in the reference system where no CNN-based QE is integrated. As can be seen, a common prediction-aware network is shared between the ILF and PP approaches. However, it is used differently, which will be explained later in this section.

##### A. QE as Post Processing (PP)

QE as PP module is placed after decoding the bitstream and before displaying the reconstructed image. Therefore, it is applicable only on the decoder side. From another point of view, pixel modifications of an image impact only the quality of that image with no temporal propagation.

In this approach, the encoder side is not aware of the fact that the displayed image will go through a QE step. Therefore, no complexity is added to the encoder and the normative aspect of the generated bitstream remains unchanged.

At the decoder side, the PP step is considered as optional. Usually, this choice depends on the processing capacity of the display device. For instance, if the device is equipped with dedicated Graphic Processing Unit (GPU) or other neural network inference hardware, then the post-processing can be applied and bring quality improvement at no bitrate cost. Another advantage of the PP approach is that it can be applied on already encoded videos without needing for their re-compression.



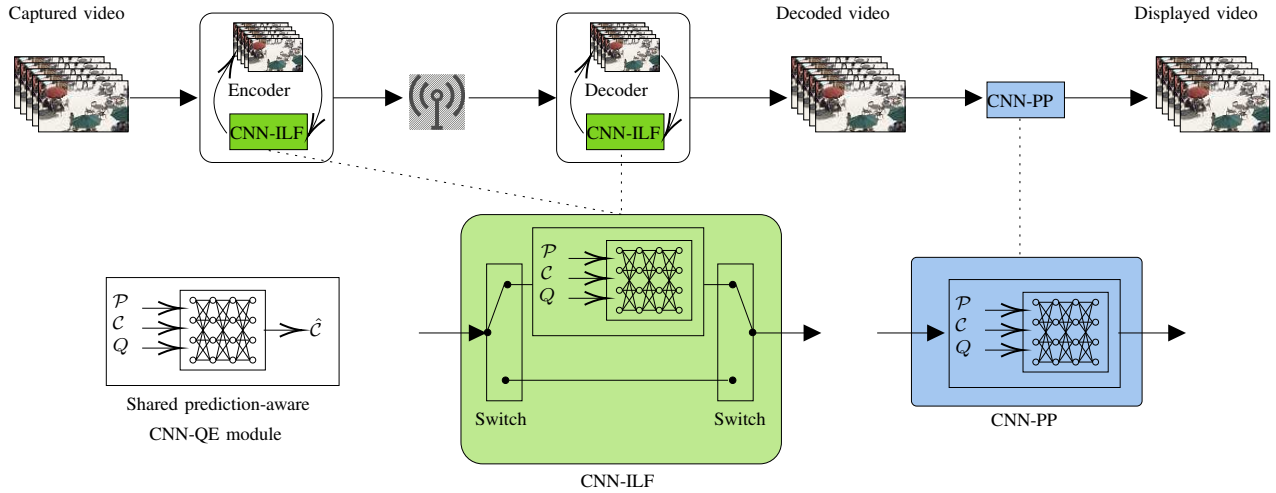


Fig. 5: The proposed prediction-aware framework with two codec integration approaches: ILF (green) and PP (blue), sharing the same CNN-based QE module.

Activating the blue box in Fig. 5 represents the scheme of the PP codec integration. As the QE module requires the necessary coding information, namely the QP map, the prediction signal and the coding type mask, which are extracted from bitstream during the decoding phase.

### B. QE as In-Loop Filter (ILF)

The main idea of an ILF is based on the propagation of improvements. More precisely, an ILF locally improves pixels of the current frame and then temporally propagates the improvement through frames which use the current frame as their reference.

QE as ILF module is placed after existing in-loop filters in VVC (*i.e.* DBF, SAO and ALF). Since the framework is shared with the PP approach, same coding information is required which is accessed during the encoding process of a frame.

Unlike the PP approach and similar to existing VVC in-loop filters, the ILF approach is normative. In other words, if activated, both encoder and decoder are forced to apply it on their reconstructed samples. Therefore, one main difference of ILF compared to the PP is the mandatory complexity at both encoder and decoder sides.

On contrary, ILF approaches have an interesting advantage of propagating the quality enhancement through the frames. Fig. 6 visualizes this aspect. In this figure, the propagation of quality enhancement in a GoP of size 8, with four temporal layers ( $Tid_i$ ,  $i=0,1,2,3$ ) is shown, where only the intra frames at POC0 and POC8 are enhanced. The offsets  $\{+1, \dots, +4\}$  approximately represents how far a frame is placed from the enhanced frames. Moreover, the spectrum of greens indicates the benefit of each frame from the enhancement propagation, based on their distance order from the enhanced intra frames. Therefore, one can see that the propagation benefit gradually diminishes as the frame gets further from the enhanced frames.

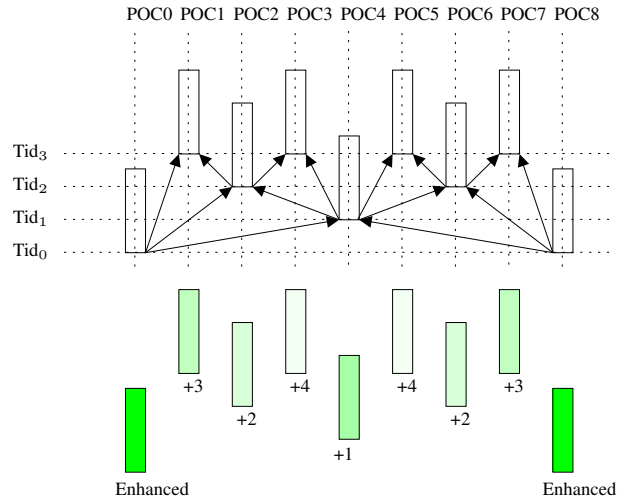


Fig. 6: Propagation of quality enhancement in ILF approach in GoP of size 8. The spectrum of greens approximately shows the benefit of each frame from the enhancement propagation, based on the distance order from the enhanced intra frames, which is approximated based on the number of steps required to reach frames from both enhanced frames.

1) *Multiple-enhancement*: The potential downside of enhancement propagation is a phenomenon called multiple enhancement in this paper. In common GoP structures with inter frames, the effect of processing one frame usually propagates through other frames that refer to it in the motion compensation. In particular, by applying in-loop quality enhancement, either CNN-based or standard methods (*e.g.* SAO, ALF, DBF etc.), when the quality of a frame in lower temporal layers is enhanced (Fig. 6), the effective enhancement will also impact frames in higher temporal layers. For instance, a reconstructed

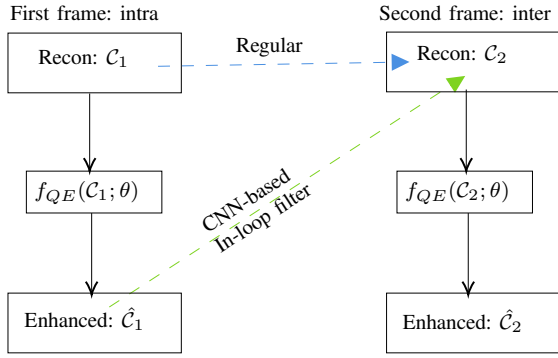


Fig. 7: Multiple enhancement example in a simplified GoP of size 2 (one intra frame at left and one inter frame at right). The dashed lines show the use of reference picture for the inter frame, with (green) and without (blue) a CNN-based in-loop filter.

inter frame, may contain blocks from its reference frames which are already enhanced by the applied method.

To better understand the multiple-enhancement effect, imagine a simplified low-delay GoP structure of length 2, with one intra frame and one inter frame (P-frame), as shown in Fig. 7. The blue and green dashed lines from the inter frame to the intra frame represent the reference frame used for its motion compensation, without and with a CNN-based ILF module, respectively. The ILF module is represented with a simplified version of Eq. (5), where the prediction signal and the QP map are not used in the enhancement, hence,  $\mathcal{I} = \mathcal{C}$ . Moreover, the reconstructed signal  $\mathcal{C}$  is composed as:

$$\mathcal{C} = \mathcal{P} + \hat{\mathcal{R}}, \quad (8)$$

where  $\mathcal{P}$  and  $\hat{\mathcal{R}}$  are the prediction signal and reconstructed residual signal (i.e. after quantization and de-quantization), respectively. Accordingly, the enhanced inter frames in Fig. 5 can be expressed as:

$$\hat{C}_2 = f_{QE}(C_2; \theta) = f_{QE}(\mathcal{P}_2 + \hat{\mathcal{R}}_2; \theta). \quad (9)$$

As often happens in content with no or limited linear motion, the residual transmission of an inter block could be skipped (i.e. the skip mode):

$$\hat{\mathcal{R}}_2 = 0. \quad (10)$$

In such circumstances, the reconstructed inter frame associated to a skip block can locally be expressed as:

$$C_2 = \mathcal{P}_2. \quad (11)$$

Since the prediction signal of the skip block is motion compensated from its enhanced reference, we also have:

$$\mathcal{P}_2 = \hat{C}_1, \quad (12)$$

which according to Eq. (9), it would result in multiple enhancement of the inter frame:

$$\hat{C}_2 = f_{QE}(\hat{C}_1; \theta) = f_{QE}(f_{QE}(C_1; \theta); \theta) \quad (13)$$

The multiple-enhancement effect is not an issue by nature. For instance, standard ILF also deal with a similar situation, where the reference frame has gone through the same enhancement process, and this multiple enhancement effect seems not to impact their performance.

However, in CNN-based QE methods, the tuning process is automatic through a complex offline training process. This aspect makes the multiple-enhancement effect a potential hazard for CNN-based ILF algorithms. More precisely, one of the main challenges is that a CNN-based QE network which is trained for the PP task, would not perform well for the ILF task, since it has not observed enhanced references during the PP training. In other words, such network has observed frames whose references were not enhanced by any CNN-based QE. While, during the ILF inference, this network will have to deal with reconstructed frames whose reference have also been enhanced by a CNN-based QE. As shown in previous studies, the multiple enhancement effect negatively impacts CNN-based ILF methods.

2) *End-to-end training solution*: One solution to the multiple-enhancement issue is to avoid the mismatch between the training set and test set. This solution, called the end-to-end training in the literature [8], guarantees that frames whose references have been through CNN-based QE are present in the training set. However, since it is important that the references of such frames are also enhanced by the same CNN-based QE, the end-to-end training solution has a potential chicken-and-egg problem.

One way to overcome the above problem is to run the dataset generation step and the training step in multiple iterations. Starting from the first temporal layer, in each iteration, one temporal layer is used for training and a network is trained for it. Then, all frames in that layer are enhanced in the dataset generation step, to be used in the training step of the next temporal layer. This solution is extremely time-consuming, therefore not practical for the current problem.

3) *Adaptive ILF method*: A greedy approach to avoid the multiple-enhancement is to determine at the encoder side whether or not a frame should be enhanced. For this purpose, an adaptive ILF mechanism for inter frames is used in the proposed method. The main idea is to enhance only frames where applying the CNN-based QE filter results in increasing the quality. More precisely, each reconstructed frame is processed by the proposed CNN-based QE method at the encoder side. Then, using the original frame as reference, an MSE comparison is performed between the unprocessed reconstructed frame (before enhancement) and the processed reconstructed frame (after enhancement). The switch in the adaptive ILF is then set based on the smaller MSE value.

The adaptive ILF solution requires an encoder-side signalling. Since in the proposed method, the encoder decides about the switch flag at the frame-level, the signalling is performed in the Picture Parameter Set (PPS). Signaling in the frame-level adds only one bit per frame, therefore, its impact on the coding efficiency is negligible. However, alternative implementations might apply the switch in finer granularity, such as CTU-level or even CU-level. This latter aspect is left as future work.

## V. EXPERIMENTAL RESULTS

### A. Experimental setup

1) *Dataset*: The training phase has been carried out under the recent Deep Neural Network Video Coding (DNNVC) Common Test Conditions (CTCs), released by JVET [71, 72]. The recommended dataset in these CTCs is BVI-DVC [73], which consists of 800 videos of 10-bit pixel representation, in different resolutions covering formats from CIF to 4K. We also used two image databases, namely DIV2K and Flickr2K for the training of intra-based networks. These datasets are composed of 900 and 2650 high quality images, respectively. The videos and images in the training dataset were converted to 10-bit YCbCr 4:2:0 and only the luma component has been used for training.

To train the models for inter frames, the native Random Access (RA) configuration of VTM10.0 reference software was used with input and internal pixel depth of 10-bit. Moreover, all in-loop filters were kept activated. The video dataset was encoded in five base QPs, {22, 27, 32, 37, 42}. For each QP, four out of 64 frames of each reconstructed video were randomly selected. Finally, a total of 3200 reconstructed frames obtained for each QP base, resulting in 16000 frames for all five QPs. The equivalent ground truth and prediction signal, as well as QP map for these reconstructed frames, were also extracted.

The networks for intra frames were trained separately by encoding the DIV2K and Flickr2K datasets in the All Intra (AI) configuration. In total, 3550 images were generated, from which we randomly selected 1200 for each QP, resulting in 5800 images. Moreover, we added the intra frames of the RA dataset to the AI dataset. To sum up, a total of 7400 intra frames were used. Finally, a patch-based strategy was employed which will be explained in Section V-A2.

For the test phase, nineteen sequences from the JVET CTCs (classes A1, A2, B, C, D and E) were used [74]. It is important to note that none of these sequences were included in the training dataset. The test sequences were finally encoded in RA and AI configurations, using the same encoder settings as for the training.

2) *Training Settings*: The networks were implemented in PyTorch platform and the training was performed on NVIDIA GeForce GTX 1080Ti GPU. The parameter  $N$  (number of residual blocks of the network) was set to 16. All networks were trained offline before encoding. The initial learning rate was set to  $10^{-5}$  with a decay of 0.5 for every 100 epochs. The Adam optimizer [75] was used for back propagation during the training and each network was trained for 500 epochs. The validation dataset was extracted from the training dataset and was composed of 50 cropped reconstructed frames and their corresponding prediction and original frames. During the training, the best network parameters were chosen based on the evaluation performed on the evaluation dataset.

The training has been performed on  $64 \times 64$  patches, randomly chosen from the training dataset. These patches are fed to the network on batches with a size of 16. Block rotation and flip were also applied randomly to selected patches to achieve data augmentation.

It is important to note that one single model is shared between the three colour components ( $Y$ ,  $U$  and  $V$ ) in all QP values. Given that the proposed method requires different models to apply the block-level coding type mask (see Section III-C), the following models should be stored at the encoder and decoder sides:

- Intra-trained model, for enhancing intra frames as well as intra blocks in inter frames.
- Inter-trained model, for enhancing inter blocks in inter frames.
- Prediction-unaware model, for enhancing skip blocks in inter frames.

3) *Evaluation metrics*: The main performance metric used for comparison is the Bjøntegaard Delta Bit Rate (BD-BR) [76]. This metric is formally interpreted as the amount of bit-rate saving in the same level of PSNR and VMAF based quality [77]. Based on this metric, the performance of the VVC reference software VTM-10.0 integrated with different configurations of the proposed CNN-based QE method is presented. For this purpose, the VTM-10.0 with no modification is used as the anchor. The BD-BR saving is calculated in two ranges of QPs,  $QP \in \{22, 27, 32, 37\}$  and  $QP \in \{27, 32, 37, 42\}$  naming CTCs QP range and high QP range, respectively.

The outputs of the tested methods are also compared in terms of Peak Signal-to-Noise Ratio (PSNR). To do so, this metric is computed for each tested CNN-based method and is noted as  $PSNR_{Prop}$ . Likewise, the metric is computed from the output of the reference anchor VTM-10, noted as  $PSNR_{VTM}$ . The original input signal before compression is used for computation of both PSNR values. The average difference between the two PSNR values, on a given set of sequences  $S$  and a set of QP values  $Q$ , is measured as the  $\Delta PSNR$  and is computed as:

$$\Delta PSNR = \frac{\sum_{s \in S} \sum_{q \in Q} (PSNR_{Prop}^{s,q} - PSNR_{VTM}^{s,q})}{|S||Q|}, \quad (14)$$

where  $|S|$  and  $|Q|$  denote the number of sequences and QP values tested, respectively. Positive values of above equation indicate compression gain. In our experiments, the presented  $\Delta PSNR$  values are averaged over four QP values of CTCs.

Finally, the relative complexity of tested methods is computed as the ratio of the Run-Time (RT) with respect to the reference. This metric, which is applicable to both encoder and decoder sides, is computed as:

$$RT = \frac{1}{|S||Q|} \sum_{s \in S} \sum_{q \in Q} \frac{RT_{Prop}^{s,q}}{RT_{VTM}^{s,q}} \quad (15)$$

### B. Ablation Study

In this section, the impact of the following elements of the proposed method are analysed: QP map training, network depth and prediction-awareness. It should be noted that for this ablation study, results and discussions are limited only to the Post Processing (PP) integration of the proposed method.

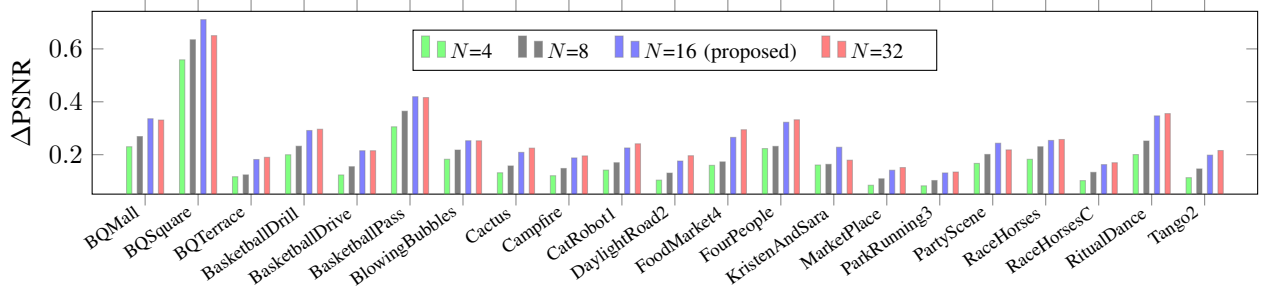


Fig. 8: Impact of the number of residual layers ( $N$ ) on the performance of the network in terms of  $\Delta$ PSNR. The reference for this test is VTM10, hence positive  $\Delta$ PSNR values indicate higher quality enhancement. All test are carried out in the RA mode.

This way, different elements of the proposed method can be evaluated without entering into the complexity of multiple-enhancement and temporal aspect of the In-Loop Filtering (ILF) integration.

1) *Network Architecture*: Generally, more complex network architectures have a larger capacity of learning complicated tasks, such as coding artifacts. In the first ablation study, we modify the network architecture, presented in Fig. 1, in terms of the number of residual blocks  $N$ . More precisely, instead of using  $N=16$ , we try alternative values 4, 8 and 32. Fig. 8 shows that decreasing the parameter  $N$  impacts the QE performance (RA configuration) in terms of  $\Delta$ PSNR. As can be seen, the global trend is a decrease in the performance. However, the difference between  $N=16$  and  $N=32$  is negligible. Therefore, in this paper we chose  $N=16$  for the network architecture.

2) *QP-map training*: QP has been used as an input to all QE networks presented in this paper. However, a noticeable number of studies in the literature take the QP-specific training approach, assuming that several trained networks can be stored at the encoder and/or decoder side.

A set of ablation studies have been conducted to understand differences between the two approaches in the All Intra (AI) coding mode. To this end, in addition to performance comparison of the two approaches, the potential damage due to the use of the incorrectly trained network in the QP-specific approach is also studied. More precisely, each network which has been trained on a particular QP was used for the QE task of other QP values.

The result is presented in Fig. 9, where the average  $\Delta$ PSNR with respect to VTM-10 is used as metric (computed on all CTCs sequences). In this figure, the proposed method based on the QP-map (shown in green) is compared to five other configurations. Four of them, expressed as  $q_L^i$  with  $i = 22, 27, 32$  and  $37$ , are the configurations where one single model trained on the QP value  $i$  is used for enhancement of all other QPs. As the fifth one, each of above models are used for their exact QP value, which results in the QP-specific methods in the literature (shown with a dashed black curve).

As can be seen, the use of QP-specific training approach is slightly better than the QP-map approach. However, the cost of storing several models makes it less useful from the

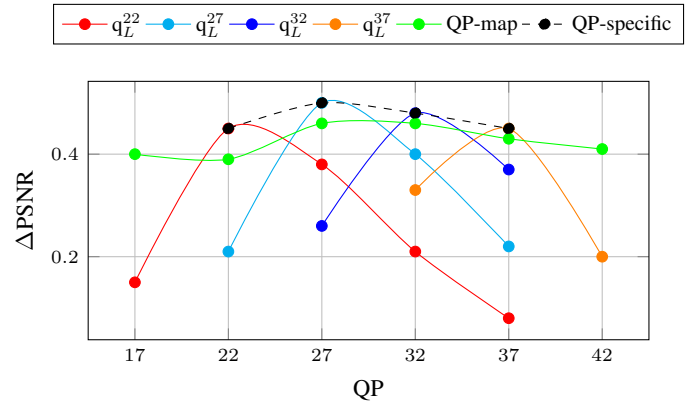


Fig. 9: PSNR performance of the QP-specific and QP-map training. The reference for the  $\Delta$ PSNR computation is VTM-10 and all test are carried out in the AI mode.

implementation point of view. Especially, this additional cost is problematic at the decoder side which is supposed to be implemented various devices with different range of capacities, including mobile devices with considerably limited hardware resources. Moreover, it can be seen that the QP-map training approach has a robust performance when applied on different QP values. On the contrary, the models that are trained for a particular QP usually have a poor performance on any other QP value, therefore, sharing them for a range of QP values can also damage the performance.

3) *Prediction-awareness*: As the main contribution, the prediction-awareness of the proposed method is evaluated in Table II, in terms of BD-BR gain compared to VTM-10. For this table, the proposed method is integrated as the PP module in the RA coding configuration. This means that both intra and inter frames have been enhanced using their dedicated networks. Moreover, the BD-BR metric is measured in two ranges of CTCs and high QPs. Finally, two configurations of the proposed QE framework are evaluated on luma and chroma components: prediction-unaware (described in Eq. (2))

and prediction-aware (described in Eq. (3)). The benchmark for the BD-BR comparison is the prediction-unaware version of the proposed CNN-based QE method.

As can be seen, the proposed prediction-aware algorithm consistently outperforms the prediction-unaware one, in both QP ranges. In the CTCs QP range, the coding gains (BD-BR(PSNR)) of prediction-awareness on  $Y$ ,  $U$  and  $V$  are -7.31% -8.90% -11.22%, respectively. Compared to the prediction-unaware setting with coding gains of -5.79%, -8.11%, -9.53%, it can be noticed that adding prediction-awareness brings -1.52%, -0.79% and -1.69% more bitrate savings in the three components, respectively. Moreover, the VMAF-based BD-BR results show even higher performance improvement when prediction information is used. Precisely, the gains for prediction-aware and prediction-unaware setting are -9.2% and -5.5%, respectively, which indicates -3.7% more bit-rate saving in terms of VMAF-based BD-BR.

Likewise, a consistent luma BD-BR gain of 1.03% by the prediction-aware compared to the prediction-unaware method can be observed in the high QP range. The relative gain in the high QP range is about 0.5% smaller than in the CTCs range. This could be explained by the fact that the absolute gains of both prediction-unaware and prediction-aware methods are larger in this QP range than in the CTCs range, possibly causing a saturation of performance gain.

### C. Performance evaluation of PP

In this section, performance of a set of recent PP methods developed for RA of VVC are compared to our proposed method. For this purpose, two academic papers [8, 60] and three JVET contributions [78–80], have been selected. The coding gain of these works is extracted from its corresponding literature. It is important to note that a fair comparison of CNN-based QE methods in the literature is difficult since they use a network with different architecture and complexity levels.

The performance of five above-mentioned methods, as well as our proposed QE, in terms of BD-BR are summarized in Table III. The average BD-BR of each class is shown for comparison. First, it can be observed that when our proposed QE is integrated as PP to the VVC, it outperforms all the competing methods. The performance improvement is consistent over the average of all classes. Secondly, the coding gain of our prediction unaware setting is less than the MFRNet [8]. It can be concluded that, by adding the same strategies to the network of MFRNet, we can even get higher coding gain. This subject will be studied in future. Finally, the work in JVET-T0079 [80] also benefits from intra prediction for enhancing the quality of intra coded frames in RA configuration. The higher BD-BR in our method compared to this work is likely due to the inter prediction and coding type mask that is employed in the proposed QE for enhancing the inter coded frames.

### D. Performance evaluation of ILF

In terms of complexity-performance trade-off, the main benefit of the ILF approach is that, due to the propagation of improvement, one can achieve higher compression gain by enhancing a few frames which are referred to the most in the

given GoP structure. In this section, we evaluate this aspect. For this reason, here a set of ILF QE configurations are defined for presenting the performance in different conditions.

1) *ILF QE configurations*: The use of sixteen frames in one GoP, as recommended in the native RA configuration of VTM, results in five temporal layers  $Tid_i$ , with  $0 \leq i \leq 4$ . For the experiments of this section, we define six ILF QE configurations, to progressively increase the number of enhanced frames in the ILF approach. In the first configuration, noted as  $C_I$ , only the intra frame in the GoP is enhanced. In each of the other five configurations, represented as  $C_j$ , with  $0 \leq j \leq 4$ , all frames in the temporal layers  $Tid_i$  (with  $i < j$ ) are enhanced (Table IV).

Additionally, we also present a configuration as  $C_{ref}$  which is equivalent to the VTM-10 encoder with no CNN-based QE and is included to be used as a reference. Using the defined ILF QE configurations, we present the results of the proposed ILF method in a progressive manner so that the impact of multiple-enhancement is reflected. For this purpose, four settings of the VTM encoder are evaluated:

- Prediction-aware ILF.
- Prediction-unaware ILF.
- Adaptive ILF (prediction-aware only).
- Prediction-aware PP.

2) *Performance Evaluation of ILF QE configurations*: Fig. 10 shows the evolution of ILF methods in different ILF QE configurations. These results are obtained by averaging over class C and D of test sequences. A constant dashed line at BD-BR=0% is shown to indicate the border between having compression gain and compression loss.

The first comparison is between the two proposed ILF methods presented with red and blue lines, for prediction-unaware and prediction-aware versions, respectively. In these versions the frame-level switch mechanism of the adaptive ILF method is not used. As can be seen, the proposed prediction-aware ILF method outperforms the prediction-unaware method in almost all configurations.

The effect of the multiple-enhancement can be seen in the shape of both prediction-unaware and prediction-aware ILF methods. More precisely, the BD-BR gain of the ILF methods progressively decreases around  $C_0$  and  $C_1$ , and eventually becomes a BD-BR loss around  $C_3$  and  $C_4$ .

As the adaptive ILF algorithm has the flexibility to apply the QE step on any arbitrary frame in the GoP, the defined ILF QE configurations are not applicable to it and its results are presented as a constant green dashed line. The only fair comparison is between the prediction-aware ILF (blue line) and the adaptive version. As can be seen, with the adaptive version we can guarantee the highest performance of the non-adaptive version. The reason behind this behaviour is that the adaptive version performs the MSE-based comparison at each frame ensures that the multiple-enhancement is not going to negatively impact the performance. Therefore, the QE task usually stops at the optimum ILF QE configuration.

The PP algorithm is adapted to the ILF QE configurations in order to make a comparison. It is important to note that such comparison with PP might not be entirely fair, as the subset of enhanced frames corresponding to given ILF QE

TABLE II: BD-BR metric for performance comparison of the proposed CNN-based QE method as Post-Processing in the RA coding configuration on top of VTM-10.0.

Class Sequence	CTCs QP (22-37)								High QP (27-42)								
	Prediction-unaware				Prediction-aware				Prediction-unaware				Prediction-aware				
	BD-BR (PSNR)			BD-BR (VMAF)	BD-BR (PSNR)			BD-BR (VMAF)	BD-BR (PSNR)			BD-BR (VMAF)	BD-BR (PSNR)			BD-BR (VMAF)	
	Y	U	V		Y	U	V		Y	U	V		Y	U	V		
A1	Tango	-5.6	-14.4	-12.5	-6.4	-8.5	-15.7	-14.5	-11.7	-6.1	-12.7	-11.7	-6.8	-7.9	-13.6	-12.8	-11.8
	FoodMarket	-3.6	-11.4	-8.4	-11.9	-7.2	-11.5	-10.5	-15.5	-5.8	-11.6	-10.0	-12.0	-7.7	-11.7	-11.0	-15.5
	CampFire	-4.3	-4.2	-10.8	-9.9	-5.9	-6.9	-14.2	-14.2	-5.9	-4.3	-10.6	-9.1	-7.4	-6.8	-13.6	-12.7
	Average	-4.5	-10.0	-10.6	-9.4	-7.2	-11.4	-13.0	-13.8	-5.9	-9.5	-10.8	-9.3	-7.7	-10.7	-12.4	-13.3
A2	CatRobot	-6.9	-13.3	-12.8	-5.4	-8.5	-13.6	-13.5	-11.1	-6.8	-11.0	-11.5	-5.7	-7.8	-11.2	-11.2	-10.9
	Daylight	-9.3	-11.3	-6.1	-9.4	-10.8	-11.5	-8.6	-15.4	-8.1	-8.8	-3.9	-9.7	-9.0	-8.8	-5.1	-15.4
	ParkRunning	-3.0	-2.6	-3.5	-1.4	-4.1	-2.4	-4.2	-5.5	-3.2	-2.7	-3.4	-1.8	-4.2	-2.9	-3.9	-5.3
	Average	-6.4	-9.1	-7.5	-5.4	-7.8	-9.2	-8.8	-10.7	-6.1	-7.5	-6.3	-5.7	-7.0	-7.6	-6.7	-10.6
B	MarketPlace	-4.8	-7.2	-8.5	-5.0	-5.6	-8.0	-9.8	-7.5	-4.6	-5.8	-9.2	-5.2	-5.2	-6.2	-10.0	-7.3
	RitualDance	-6.0	-9.0	-11.3	-8.5	-8.0	-10.6	-13.4	-11.7	-6.2	-8.0	-12.5	-8.3	-7.6	-9.0	-13.8	-11.2
	Cactus	-4.2	-6.3	-8.5	-6.3	-6.0	-6.3	-10.2	-8.6	-5.5	-5.9	-9.3	-6.4	-6.7	-6.0	-10.3	-8.5
	BasketballDrive	-5.4	-6.8	-13.4	-3.9	-7.0	-10.1	-15.3	-7.3	-5.8	-2.2	-13.4	-4.7	-7.0	-9.4	-14.4	-7.7
	BQTerrace	-4.9	-11.8	-9.9	1.3	-5.9	-13.3	-12.8	-2.9	-6.7	-7.7	-6.6	0.1	-7.4	-8.4	-7.6	-3.3
	Average	-5.1	-8.2	-10.3	-4.5	-6.5	-9.7	-12.3	-7.6	-5.8	-5.9	-10.2	-4.9	-6.8	-7.8	-11.2	-7.6
C	BasketballDrill	-6.5	-12.0	-15.3	-6.4	-8.3	-12.3	-16.3	-9.4	-6.6	-10.2	-16.3	-6.4	-7.9	-10.8	-15.8	-9.2
	BQMall	-5.2	-5.2	-6.4	-4.9	-6.7	-5.5	-7.4	-8.7	-6.4	-3.7	-6.6	-5.0	-7.2	-4.0	-6.9	-8.4
	PartyScene	-5.3	-4.7	-7.3	-3.9	-6.1	-4.8	-8.2	-7.5	-5.9	-3.6	-6.6	-4.0	-6.3	-3.8	-6.7	-7.0
	Average	-5.0	-7.6	-9.4	-4.8	-6.3	-8.0	-10.9	-8.2	-5.6	-6.6	-9.7	-4.9	-6.6	-7.1	-10.3	-7.9
D	BasketballPass	-8.0	-7.5	-16.6	-7.2	-8.9	-7.9	-17.2	-10.0	-9.0	-6.3	-16.8	-6.7	-9.4	-6.8	-16.8	-9.2
	BQSquare	-12.4	-3.8	-5.9	1.1	-12.8	-4.3	-6.8	-2.4	-12.8	-0.5	-3.7	0.1	-12.9	-1.2	-4.2	-2.8
	BlowingBubble	-6.2	-5.3	-6.6	-7.3	-7.0	-5.9	-8.4	-9.2	-6.6	-3.6	-4.7	-6.7	-7.5	-4.3	-6.2	-8.4
	Average	-8.0	-6.4	-9.4	-4.9	-9.0	-6.8	-10.7	-7.5	-8.5	-4.6	-8.5	-4.7	-9.2	-5.2	-9.1	-6.9
<b>All</b>	<b>-5.8</b>	<b>-8.1</b>	<b>-9.5</b>	<b>-5.5</b>	<b>-7.3</b>	<b>-8.9</b>	<b>-11.2</b>	<b>-9.2</b>	<b>-6.4</b>	<b>-6.6</b>	<b>-9.2</b>	<b>-5.7</b>	<b>-7.4</b>	<b>-7.5</b>	<b>-10.1</b>	<b>-8.9</b>	

TABLE III: BD-BR comparison of the proposed method against state-of-the-art PP methods. All tests have been carried out in the RA mode and under JVET-CTCs.

Class	State-of-the-art					Proposed	
	JVET-O0132 [78]	JVET-O0079 [79]	Zhang <i>et al.</i> [52]	JVET-T0079 [80]	MFRNet [8]	Pred-unaware	Pred-aware
	VTM-4	VTM-5	VTM-4	VTM-10	VTM-7	VTM-10	VTM-10
A1	-0.15%	-0.87%	-2.41%	-2.86%	-6.73%	-4.47%	-7.20%
A2	-0.28%	-1.68%	-4.22%	-2.98%	-7.16%	-6.41%	-7.79%
B	-0.22%	-1.47%	-2.57%	-2.92%	-6.30%	-5.06%	-6.50%
C	-0.59%	-3.34%	-3.89%	-2.96%	-6.00%	-4.97%	-6.35%
D	-0.80%	-4.97%	-5.80%	-3.48%	-7.60%	-8.04%	-9.01%
<b>All</b>	<b>-0.40%</b>	<b>-2.47%</b>	<b>-3.76%</b>	<b>-3.04%</b>	<b>-6.70%</b>	<b>-5.79%</b>	<b>-7.31%</b>

TABLE IV: Description of the tested ILF QE configurations used for evaluation of the ILF approach. In each configuration, frames in some temporal layer of the GoP are enhanced (✓) and some are not enhanced (✗). All tests are carried out in the RA mode.

Temporal layer ID	ILF QE configuration						
	Ref	C <sub>1</sub>	C <sub>0</sub>	C <sub>1</sub>	C <sub>2</sub>	C <sub>3</sub>	C <sub>4</sub>
Intra	✗	✓	✓	✓	✓	✓	✓
0	✗	✗	✓	✓	✓	✓	✓
1	✗	✗	✗	✓	✓	✓	✓
2	✗	✗	✗	✗	✓	✓	✓
3	✗	✗	✗	✗	✗	✓	✓
4	✗	✗	✗	✗	✗	✗	✓

configurations are not necessarily optimal subsets for PP. However, our experiments show that the difference is small enough for drawing a conclusion. The interesting comparison between the PP method and the two ILF methods is their crossing point. In other words, until around  $C_2$ , both ILF methods are better than the PP. However, after this configuration, the PP becomes better. The reason is that, in the first part (until  $C_2$ , the enhancement propagation is causing the ILF methods to be better than the PP. However, in the second part ( $C_3$  and  $C_4$ ), the negative impact of the multiple-enhancement effect entirely compensates the enhancement propagation effect. Therefore, the crossing point of the PP method and ILF methods shows how the balance between the enhancement propagation and the multiple-enhancement can impact the performance of ILF method.

The final observation from Fig. 10 is the fact that best per-

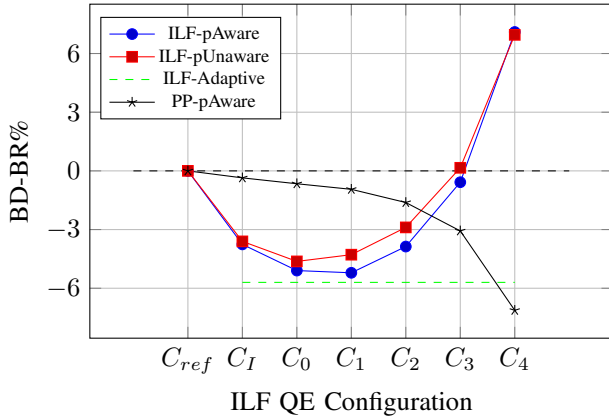


Fig. 10: Performance evaluation of different ILF QE configurations of the ILF approach, in terms of BD-BR. The proposed prediction-aware PP performance is also presented (black line) in order to magnify the performance drop due to the multiple enhancement effect in the last configurations of the ILF approach. All tests are carried out in the RA mode (Class C and D, CTC).

formance of the PP (at  $C_4$ ) is better than the best performance of the ILF (shown with ILF-Adaptive line). This is most likely due to the fact that current ILF methods are not optimized with end-to-end training to be able to enhance frames in higher temporal layers (e.g. at  $C_3$  and  $C_4$ ). Improvement of this aspect is left as future work.

3) *Performance vs Complexity Trade-off*: In general, by applying the ILF approach to the frames in lower temporal layers, the side effect of multiple enhancement can be controlled. For instance, if only first I frame is enhanced and other frames remain intact, a noticeable gain will be obtained compared to the fact that only one frame is enhanced. In other words, by imposing the complexity of enhancing only one frame, we obtain a good portion of performance if we apply QE to all frames. To test this effect, we have calculated in table V the relative complexity of the configurations introduced in section V-D1. As can be seen, the encoding and decoding time is increasing as we apply QE filter to more temporal levels.

We can also see from Table V-D1 that, the decoder complexity of ILF in the adaptive configuration ( $C_{ad}$ ) varies depending on how many frames have been enhanced at the encoder side. On the other hand, using PP does not impose any complexity at the encoder side, however at the decoder side, it dramatically increases the complexity.

4) *Performance comparison with state-of-the-art of ILF*: Table VI compares the performance of proposed QE methods, when integrated as ILF, against some state-of-the-art methods in literature. For this purpose, we chose MFRNet [8] and ADCNN [27] methods from academic papers in addition to three recent JVET contributions. As the source code of most of these works is not publicly available, the performance metric have been directly extracted from corresponding papers and documents. For representing both prediction-unaware and

prediction-aware methods, we used the adaptive ILF implementation, described in Section IV-B3, since it provides the highest performance.

It can be observed that our proposed prediction-aware ILF outperforms the proposed prediction-unaware method, by the coding gain of -5.85% compared to -5.12%, showing a consistent average BD-BR gain of about -0.73%. This result shows once more how the use of the prediction information can further improve the performance of a given CNN-based QE method.

Furthermore, the proposed prediction-aware method also significantly outperforms the selected papers from the state-of-the-art. It is worth to mention that since the benchmark methods use different network architecture and sometimes different training and test settings, this comparison might not entirely be fair. As future work, more efficient network architectures can be adopted from some of the benchmarks methods and integrated into the proposed prediction-aware framework of this paper. Or inversely, one can implement the prediction-aware aspect of the proposed method on top of the benchmark methods and measure its performance changes.

In another analysis, the ILF results of Table VI can be compared against the PP results in Table III. By doing so, it can be observed that the PP approach is -1.4% better than the ILF one. This is mainly due to the multiple enhancement effect and the fact the CNN-based enhancement in some high temporal layers in the GoP have been avoided by the adaptive mechanism of the proposed method in order to control the quality degradation.

## VI. CONCLUSION

In this paper, we have proposed a CNN-based QE method to address the Post Processing (PP) and In-Loop Filtering (ILF) problems in VVC. Precisely, a filter which exploits the coding information such as prediction and QP is proposed in order to better enhance the quality. These coding information is fed to a proposed QE network based on the frame coding type (intra-frame or inter-frame), resulting in several trained models. Depending on the coding type used for a block (e.g inter mode, intra mode or skip mode), a model is selected among three models for the QE task. Moreover, in the ILF integration, in order to avoid the multiple enhancement issue, we adopt an adaptive framework to skip enhancement of frames posing this problem. Experimental results showed that the proposed PP, as well as ILF methods, outperform the state-of-art methods in terms of BD-BR.

There are rooms for improvement of this work. For instance, the proposed QE framework enhances all three components using one single model for a given coding type. However, the content of chroma components has different characteristics which could be taken into account separately, during the training and inference. Moreover, there is plenty of coding information available during the encoding and within the bitstream at the decoder side. This coding information could provide a variety of spatial and temporal features from the video. The promising improvement we achieved from using the prediction signal and QP is encouraging to deeper investigate

TABLE V: Relative Complexity of the proposed PP and ILF, averaged on CTCs QP range, as in Eq. (15). Here,  $C_i$  refers to the ILF configurations presented in section V-D2. All tests have been carried out with the native RA coding mode of VTM-10.

Platform	Class	PP		ILF - $C_{ad}$		ILF - $C_I$		ILF - $C_0$		ILF - $C_1$		ILF - $C_2$		ILF - $C_3$	
		ET	DT	ET	DT	ET	DT	ET	DT	ET	DT	ET	DT	ET	DT
CPU	B	-	96.82	1.08	37.18	1.00	3.95	1.01	8.37	1.01	14.27	1.02	26.06	1.04	48.50
	C	-	329.87	1.17	78.76	1.01	12.27	1.01	26.30	1.02	46.54	1.05	87.01	1.09	167.96
	D	-	312.71	1.21	90.17	1.01	11.58	1.02	24.98	1.03	44.16	1.05	82.53	1.10	159.25
GPU	B	-	25.06	1.02	4.15	1.00	1.74	1.00	2.85	1.00	4.33	1.01	7.29	1.01	12.92
	C	-	14.36	1.01	2.6	1.00	1.46	1.00	2.03	1.00	2.85	1.00	4.49	1.00	7.78
	D	-	13.61	1.04	3.5	1.00	1.38	1.01	1.93	1.01	2.70	1.00	4.26	1.01	7.38

TABLE VI: BD-BR comparison of the proposed ILF method against state-of-the-art methods, computed on the RA mode.

Class	State-of-the-art						Proposed	
	JVET-O0079 [79] VTM-5	JVET-T0088 [81] VTM-9	JVET-U0054 [82] VTM-10	MFRNet [8] VTM-7	ADCNN [27] VTM-4	JVET-T0079 [80] VTM-10	Pred-unaware VTM-10	Pred-aware VTM-10
B	0.64%	-3.44%	-4.04%	-4.30%	-1.53%	-3.25%	-5.12%	-5.85%
C	-1.17%	-3.38%	-4.69%	-3.30%	-3.06%	-2.85%	-4.36%	-5.13%
D	-3.13%	-3.48%	-6.20%	-5.50%	-3.83%	-3.13%	-5.87%	-6.58%
All	<b>-1.22%</b>	<b>-3.43%</b>	<b>-4.98%</b>	<b>-4.37%</b>	<b>-2.81%</b>	<b>-3.08%</b>	<b>-5.12%</b>	<b>-5.85%</b>

the effect of other coding information. Therefore, as another future work, one can benefit from other coding information for further improving the proposed QE framework. Finally, the network can be further simplified by using more efficient architecture in order to decrease the number of parameters, leading to a faster inference.

#### REFERENCES

- [1] B. Bross, J. Chen, S. Liu, and Y.-K. Wang, "Versatile video coding (draft 7)," in *JVET-P2001, Geneva, Switzerland*, October 2019.
- [2] AOMedia Video 1 (AV1), "https://aomedia.google.com/."
- [3] K. Choi, J. Chen, D. Rusanovskyy, K.-P. Choi, and E. S. Jang, "An overview of the MPEG-5 essential video coding standard [standards in a nutshell]," *IEEE Signal Processing Magazine*, vol. 37, no. 3, pp. 160–167, 2020.
- [4] G. J. Sullivan, J.-R. Ohm, W.-J. Han, and T. Wiegand, "Overview of the high efficiency video coding (HEVC) standard," *IEEE Transactions on circuits and systems for video technology*, vol. 22, no. 12, pp. 1649–1668, 2012.
- [5] M. Karczewicz, N. Hu, J. Taquet, C.-Y. Chen, K. Misra, K. Andersson, P. Yin, T. Lu, E. François, and J. Chen, "VVC in-loop filters," *IEEE Transactions on Circuits and Systems for Video Technology*, 2021.
- [6] D. Liu, Y. Li, J. Lin, H. Li, and F. Wu, "Deep learning-based video coding: A review and a case study," *ACM Computing Surveys (CSUR)*, vol. 53, no. 1, pp. 1–35, 2020.
- [7] S. Ma, X. Zhang, C. Jia, Z. Zhao, S. Wang, and S. Wang, "Image and video compression with neural networks: A review," *IEEE Transactions on Circuits and Systems for Video Technology*, vol. 30, no. 6, pp. 1683–1698, 2019.
- [8] D. Ma, F. Zhang, and D. Bull, "MFRNet: a new CNN architecture for post-processing and in-loop filtering," *IEEE Journal of Selected Topics in Signal Processing*, 2020.
- [9] J. Yao and L. Wang, "Convolutional neural network filter (CNNF) for intra frame," in *JVET-N0169, Geneva, Switzerland*, 2019.
- [10] J. Kang, S. Kim, and K. M. Lee, "Multi-modal/multi-scale convolutional neural network based in-loop filter design for next generation video codec," in *2017 IEEE International Conference on Image Processing (ICIP)*, pp. 26–30, IEEE, 2017.
- [11] X. He, Q. Hu, X. Zhang, C. Zhang, W. Lin, and X. Han, "Enhancing HEVC compressed videos with a partition-masked convolutional neural network," in *2018 25th IEEE International Conference on Image Processing (ICIP)*, pp. 216–220, IEEE, 2018.
- [12] M. Wang, S. Wan, H. Gong, Y. Yu, and Y. Liu, "An integrated CNN-based post processing filter for intra frame in versatile video coding," in *2019 Asia-Pacific Signal and Information Processing Association Annual Summit and Conference (APSIPA ASC)*, pp. 1573–1577, IEEE, 2019.
- [13] W.-S. Park and M. Kim, "CNN-based in-loop filtering for coding efficiency improvement," in *2016 IEEE 12th Image, Video, and Multidimensional Signal Processing Workshop (IVMSP)*, pp. 1–5, IEEE, 2016.
- [14] C. Jia, S. Wang, X. Zhang, S. Wang, and S. Ma, "Spatial-temporal residue network based in-loop filter for video coding," in *2017 IEEE Visual Communications and Image Processing (VCIP)*, pp. 1–4, IEEE, 2017.
- [15] T. Wang, M. Chen, and H. Chao, "A novel deep learning-based method of improving coding efficiency from the decoder-end for HEVC," in *2017 Data Compression Conference (DCC)*, pp. 410–419, IEEE, 2017.
- [16] R. Yang, M. Xu, and Z. Wang, "Decoder-side HEVC quality enhancement with scalable convolutional neural network," in *2017 IEEE International Conference on*



- Multimedia and Expo (ICME)*, pp. 817–822, IEEE, 2017.
- [17] Y. Dai, D. Liu, and F. Wu, “A convolutional neural network approach for post-processing in HEVC intra coding,” in *International Conference on Multimedia Modeling*, pp. 28–39, Springer, 2017.
- [18] T. Wang, W. Xiao, M. Chen, and H. Chao, “The multi-scale deep decoder for the standard HEVC bitstreams,” in *2018 Data Compression Conference*, pp. 197–206, IEEE, 2018.
- [19] R. Yang, M. Xu, T. Liu, Z. Wang, and Z. Guan, “Enhancing quality for HEVC compressed videos,” *IEEE Transactions on Circuits and Systems for Video Technology*, vol. 29, no. 7, pp. 2039–2054, 2018.
- [20] J. W. Soh, J. Park, Y. Kim, B. Ahn, H.-S. Lee, Y.-S. Moon, and N. I. Cho, “Reduction of video compression artifacts based on deep temporal networks,” *IEEE Access*, vol. 6, pp. 63094–63106, 2018.
- [21] R. Yang, M. Xu, Z. Wang, and T. Li, “Multi-frame quality enhancement for compressed video,” in *Proceedings of the IEEE Conference on Computer Vision and Pattern Recognition*, pp. 6664–6673, 2018.
- [22] X. Song, J. Yao, L. Zhou, L. Wang, X. Wu, D. Xie, and S. Pu, “A practical convolutional neural network as loop filter for intra frame,” in *2018 25th IEEE International Conference on Image Processing (ICIP)*, pp. 1133–1137, IEEE, 2018.
- [23] Y. Zhang, T. Shen, X. Ji, Y. Zhang, R. Xiong, and Q. Dai, “Residual highway convolutional neural networks for in-loop filtering in HEVC,” *IEEE Transactions on image processing*, vol. 27, no. 8, pp. 3827–3841, 2018.
- [24] F. Li, W. Tan, and B. Yan, “Deep residual network for enhancing quality of the decoded intra frames of HEVC,” in *2018 25th IEEE International Conference on Image Processing (ICIP)*, pp. 3918–3922, IEEE, 2018.
- [25] L. Ma, Y. Tian, and T. Huang, “Residual-based video restoration for HEVC intra coding,” in *2018 IEEE Fourth International Conference on Multimedia Big Data (BigMM)*, pp. 1–7, IEEE, 2018.
- [26] X. Meng, X. Deng, S. Zhu, S. Liu, C. Wang, C. Chen, and B. Zeng, “Mganet: A robust model for quality enhancement of compressed video,” *arXiv preprint arXiv:1811.09150*, 2018.
- [27] M.-Z. Wang, S. Wan, H. Gong, and M.-Y. Ma, “Attention-based dual-scale CNN in-loop filter for versatile video coding,” *IEEE Access*, vol. 7, pp. 145214–145226, 2019.
- [28] D. Wang, S. Xia, W. Yang, Y. Hu, and J. Liu, “Partition tree guided progressive rethinking network for in-loop filtering of HEVC,” in *2019 IEEE International Conference on Image Processing (ICIP)*, pp. 2671–2675, IEEE, 2019.
- [29] X. Meng, X. Deng, S. Zhu, and B. Zeng, “Enhancing quality for VVC compressed videos by jointly exploiting spatial details and temporal structure,” in *2019 IEEE International Conference on Image Processing (ICIP)*, pp. 1193–1197, IEEE, 2019.
- [30] H. Zhao, M. He, G. Teng, X. Shang, G. Wang, and Y. Feng, “A CNN-based post-processing algorithm for video coding efficiency improvement,” *IEEE Access*, vol. 8, pp. 920–929, 2019.
- [31] T. Li, M. Xu, C. Zhu, R. Yang, Z. Wang, and Z. Guan, “A deep learning approach for multi-frame in-loop filter of HEVC,” *IEEE Transactions on Image Processing*, vol. 28, no. 11, pp. 5663–5678, 2019.
- [32] L. Yu, L. Shen, H. Yang, L. Wang, and P. An, “Quality enhancement network via multi-reconstruction recursive residual learning for video coding,” *IEEE Signal Processing Letters*, vol. 26, no. 4, pp. 557–561, 2019.
- [33] S. Zhang, Z. Fan, N. Ling, and M. Jiang, “Recursive residual convolutional neural network-based in-loop filtering for intra frames,” *IEEE Transactions on Circuits and Systems for Video Technology*, 2019.
- [34] T. M. Hoang and J. Zhou, “B-DRRN: A block information constrained deep recursive residual network for video compression artifacts reduction,” in *2019 Picture Coding Symposium (PCS)*, pp. 1–5, IEEE, 2019.
- [35] L. Feng, X. Zhang, S. Wang, Y. Wang, and S. Ma, “Coding prior based high efficiency restoration for compressed video,” in *2019 IEEE International Conference on Image Processing (ICIP)*, pp. 769–773, IEEE, 2019.
- [36] G. Chen, D. Ding, D. Mukherjee, U. Joshi, and Y. Chen, “AV1 in-loop filtering using a wide-activation structured residual network,” in *2019 IEEE International Conference on Image Processing (ICIP)*, pp. 1725–1729, IEEE, 2019.
- [37] Y. Bei, Q. Wang, Z. Cheng, X. Pan, J. Lei, L. Wang, and D. Ding, “A CU-level adaptive decision method for CNN-based in-loop filtering,” in *Eleventh International Conference on Graphics and Image Processing (ICGIP 2019)*, vol. 11373, p. 113731G, International Society for Optics and Photonics, 2020.
- [38] R. Yang, X. Sun, M. Xu, and W. Zeng, “Quality-gated convolutional LSTM for enhancing compressed video,” in *2019 IEEE International Conference on Multimedia and Expo (ICME)*, pp. 532–537, IEEE, 2019.
- [39] G. Lu, X. Zhang, W. Ouyang, D. Xu, L. Chen, and Z. Gao, “Deep non-local kalman network for video compression artifact reduction,” *IEEE Transactions on Image Processing*, vol. 29, pp. 1725–1737, 2019.
- [40] D. Ding, G. Chen, D. Mukherjee, U. Joshi, and Y. Chen, “A CNN-based in-loop filtering approach for av1 video codec,” in *2019 Picture Coding Symposium (PCS)*, pp. 1–5, IEEE, 2019.
- [41] J. Tong, X. Wu, D. Ding, Z. Zhu, and Z. Liu, “Learning-based multi-frame video quality enhancement,” in *2019 IEEE International Conference on Image Processing (ICIP)*, pp. 929–933, IEEE, 2019.
- [42] M. Lu, T. Chen, H. Liu, and Z. Ma, “Learned image restoration for VVC intra coding,” in *CVPR Workshops*, p. 0, 2019.
- [43] D. Ding, L. Kong, G. Chen, Z. Liu, and Y. Fang, “A switchable deep learning approach for in-loop filtering in video coding,” *IEEE Transactions on Circuits and Systems for Video Technology*, 2019.
- [44] X. Xu, J. Qian, L. Yu, H. Wang, X. Zeng, Z. Li, and N. Wang, “Dense inception attention neural network for in-loop filter,” in *2019 Picture Coding Symposium (PCS)*,

- pp. 1–5, IEEE, 2019.
- [45] C. Jia, S. Wang, X. Zhang, S. Wang, J. Liu, S. Pu, and S. Ma, “Content-aware convolutional neural network for in-loop filtering in high efficiency video coding,” *IEEE Transactions on Image Processing*, vol. 28, no. 7, pp. 3343–3356, 2019.
- [46] Z. Pan, X. Yi, Y. Zhang, B. Jeon, and S. Kwong, “Efficient in-loop filtering based on enhanced deep convolutional neural networks for HEVC,” *IEEE Transactions on Image Processing*, vol. 29, pp. 5352–5366, 2020.
- [47] X. Meng, X. Deng, S. Zhu, and B. Zeng, “Bstn: An effective framework for compressed video quality enhancement,” in *2020 IEEE Conference on Multimedia Information Processing and Retrieval (MIPR)*, pp. 320–325, IEEE, 2020.
- [48] X. Meng, X. Deng, S. Zhu, S. Liu, and B. Zeng, “Flow-guided temporal-spatial network for HEVC compressed video quality enhancement,” in *2020 Data Compression Conference (DCC)*, pp. 384–384, IEEE, 2020.
- [49] W.-G. Chen, R. Yu, and X. Wang, “Neural network-based video compression artifact reduction using temporal correlation and sparsity prior predictions,” *IEEE Access*, 2020.
- [50] Y.-H. Lam, A. Zare, F. Cricri, J. Lainema, and M. Hanuksela, “Efficient adaptation of neural network filter for video compression,” *arXiv preprint arXiv:2007.14267*, 2020.
- [51] H. Huang, I. Schiopu, and A. Munteanu, “Frame-wise CNN-based filtering for intra-frame quality enhancement of HEVC videos,” *IEEE Transactions on Circuits and Systems for Video Technology*, 2020.
- [52] F. Zhang, C. Feng, and D. R. Bull, “Enhancing VVC through CNN-based post-processing,” in *2020 IEEE International Conference on Multimedia and Expo (ICME)*, pp. 1–6, IEEE, 2020.
- [53] Q. Xing, M. Xu, T. Li, and Z. Guan, “Early Exit Or Not: Resource-efficient blind quality enhancement for compressed images,” *arXiv preprint arXiv:2006.16581*, 2020.
- [54] W. Sun, X. He, H. Chen, R. E. Sheriff, and S. Xiong, “A quality enhancement framework with noise distribution characteristics for high efficiency video coding,” *Neurocomputing*, vol. 411, pp. 428–441, 2020.
- [55] H. Li, W. Lei, and W. Zhang, “QEVC: Quality enhancement-oriented video coding,” in *2020 5th International Conference on Computer and Communication Systems (ICCCS)*, pp. 296–300, IEEE, 2020.
- [56] X. Li, S. Sun, Z. Zhang, and Z. Chen, “Multi-scale grouped dense network for VVC intra coding,” in *Proceedings of the IEEE/CVF Conference on Computer Vision and Pattern Recognition Workshops*, pp. 158–159, 2020.
- [57] D. Ding, W. Wang, J. Tong, X. Gao, Z. Liu, and Y. Fang, “Biprediction-based video quality enhancement via learning,” *IEEE transactions on cybernetics*, 2020.
- [58] J. Wang, X. Deng, M. Xu, C. Chen, and Y. Song, “Multi-level wavelet-based generative adversarial network for perceptual quality enhancement of compressed video,” *arXiv preprint arXiv:2008.00499*, 2020.
- [59] X. Xu, J. Qian, L. Yu, H. Wang, H. Tao, and S. Yu, “Spatial-temporal fusion convolutional neural network for compressed video enhancement in HEVC,” in *2020 Data Compression Conference (DCC)*, pp. 402–402, IEEE, 2020.
- [60] Z. Jin, P. An, C. Yang, and L. Shen, “Post-processing for intra coding through perceptual adversarial learning and progressive refinement,” *Neurocomputing*, vol. 394, pp. 158–167, 2020.
- [61] T. Wang, J. He, S. Xiong, P. Karn, and X. He, “Visual perception enhancement for HEVC compressed video using a generative adversarial network,” in *2020 International Conference on UK-China Emerging Technologies (UCET)*, pp. 1–4, IEEE, 2020.
- [62] V. Nair and G. E. Hinton, “Rectified linear units improve restricted boltzmann machines,” in *Icml*, 2010.
- [63] S. Ioffe and C. Szegedy, “Batch normalization: Accelerating deep network training by reducing internal covariate shift,” in *International conference on machine learning*, pp. 448–456, PMLR, 2015.
- [64] Z. Guan, Q. Xing, M. Xu, R. Yang, T. Liu, and Z. Wang, “MFQE 2.0: A new approach for multi-frame quality enhancement on compressed video,” *IEEE Transactions on Pattern Analysis and Machine Intelligence*, 2019.
- [65] E. Ilg, N. Mayer, T. Saikia, M. Keuper, A. Dosovitskiy, and T. Brox, “Flownet 2.0: Evolution of optical flow estimation with deep networks,” in *Proceedings of the IEEE conference on computer vision and pattern recognition*, pp. 2462–2470, 2017.
- [66] F. Nasiri, W. Hamidouche, L. Morin, N. Dhollande, and G. Cocherel, “Prediction-aware quality enhancement of VVC using CNN,” in *2020 IEEE International Conference on Visual Communications and Image Processing (VCIP)*, pp. 310–313, IEEE, 2020.
- [67] G. Lu, W. Ouyang, D. Xu, X. Zhang, Z. Gao, and M.-T. Sun, “Deep kalman filtering network for video compression artifact reduction,” in *Proceedings of the European Conference on Computer Vision (ECCV)*, pp. 568–584, 2018.
- [68] B. Lim, S. Son, H. Kim, S. Nah, and K. Mu Lee, “Enhanced deep residual networks for single image super-resolution,” in *Proceedings of the IEEE conference on computer vision and pattern recognition workshops*, pp. 136–144, 2017.
- [69] F. Nasiri, W. Hamidouche, L. Morin, G. Cocherel, and N. Dhollande, “A study on the impact of training data in CNN-based super-resolution for low bitrate end-to-end video coding,” in *2020 Tenth International Conference on Image Processing Theory, Tools and Applications (IPTA)*, pp. 1–5, IEEE, 2020.
- [70] F. Nasiri, W. Hamidouche, L. Morin, G. Cocherel, and N. Dhollande, “Model selection CNN-based VVC quality enhancement,” in *2021 Picture Coding Symposium (PCS)*, pp. 1–5, 2021.
- [71] S. Liu, A. Segall, E. Alshina, and R.-L. Liao, “JVET common test conditions and evaluation procedures for neural network-based video coding technology,” in *JVET*

*T2006, Teleconference*, 2020.

- [72] E. Alshina, A. Segall, R.-L. Liao, and T. Solovyev, “[DNNVC] comments on common test conditions and reporting template,” in *JVET-T0129, Teleconference*, 2020.
- [73] D. Ma, F. Zhang, and D. R. Bull, “BVI-DVC: a training database for deep video compression,” *arXiv preprint arXiv:2003.13552*, 2020.
- [74] F. Bossen, J. Boyce, K. Suehring, X. Li, and V. Seregin, “JVET common test conditions and software reference configurations for SDR video,” in *JVET-N1010, Geneva, Switzerland*, 2019.
- [75] D. P. Kingma and J. Ba, “Adam: A method for stochastic optimization,” *arXiv preprint arXiv:1412.6980*, 2014.
- [76] G. Bjontegaard, “Improvement of BD-PSNR model,” *Document VCEG-A111*, Berlin, Germany, July 2008.
- [77] Z. Li, A. Aaron, I. Katsavounidis, A. Moorthy, and M. M. Manohara, “Toward a practical perceptual video quality metric,” in *The Netflix Tech Blog, vol. 6*, pp. 149–152, Netflix, 2016.
- [78] Y. Kidani, K. Kawamura, K. Unno, and S. Naito, “Evaluation results of CNN-based filtering with off-line learning model,” in *JVET-O0132, Gothenburg, Sweden*, 2019.
- [79] S. Wan, M. Wang, Y. Ma, J. Huo, H. Gong, C. Zou, Y. Yu, and Y. Liu, “Integrated in-loop filter based on CNN,” in *JVET-O0079, Gothenburg, Sweden*, 2019.
- [80] H. Wang, M. Karczewicz, J. Chen, and A. Meher Kotra, “AHG11: Neural network-based in-loop filter,” in *JVET-T0079, Teleconference*, 2020.
- [81] Y. Li, L. Zhang, K. Zhang, Y. He, and J. Xu, “AHG11: Convolutional neural networks-based in-loop filter,” in *JVET-T0088, Teleconference*, 2020.
- [82] Z. Wang, R.-L. Liao, C. Ma, and Y. Ye, “EE-1.6: Neural network based in-loop filtering,” in *JVET-U0054, Teleconference*, 2021.